ICOEST 2025 Sarajevo

11TH INTERNATIONAL CONFERENCE ON ENVIRONMENTAL SCIENCE AND TECHNOLOGY

October 22-26, 2025

BOOK OF PROCEEDINGS

www.icoest.eu

Organized by

ORGANIZERS

Partners

11th INTERNATIONAL CONFERENCE ON ENVIRONMENTAL SCIENCE AND TECHNOLOGY (ICOEST)

ISBN 978-605-81426-2-6

ISSN – 2687-2439

BOOK OF PROCEEDINGS OF THE 11th INTERNATIONAL CONFERENCE ON ENVIRONMENTAL SCIENCE AND TECHNOLOGY (ICOEST)
SARAJEVO, BOSNIA AND HERZEGOVINA on October 22-26, 2025

Edited by

Prof. Dr. Özer Çınar

Published by:

info@icoest.eu
www.icoest.eu
www.cnrgroup.eu

CNR Group Laboratuvar ve Arge Hizmetleri Sanayi Ticaret Limited Şirketi Çifte Havuzlar Mah., Eski Londra Asfaltı Cad., Kuluçka Mrk., A1 Blok, 151/1C, Iç Kapı No:1 B-20, Esenler / Istanbul, 34220

SCIENTIFIC COMMITTEE

1. Prof.Dr. Adisa Parić - University of Sarajevo - Bosnia and Herzegovina
2. Prof.Dr. Ana Vovk-Korže - University of Maribor - Slovenia
3. Prof.Dr. Ayşegül Pala - Dokuz Eylül University - Turkey
4. Prof.Dr. Cevat Yaman - Imam Abdulrahman Bin Faisal University - Saudi Arabia
5. Prof.Dr. Cumali Kınacı - İstanbul Technical University - Turkey
6. Prof.Dr. Dragan Vinterhalter - University of Belgrade - Serbia
7. Prof.Dr. Dragutin T. Mihailović - University of Novi Sad - Serbia
8. Prof.Dr. Edina Muratović - University of Sarajevo - Bosnia and Herzegovina
9. Prof.Dr. Esad Prohic - University of Zagreb - Croatia
10. Prof.Dr. Hasan Merdun - Akdeniz University - Turkey
11. Prof.Dr. Jasna Huremović - University of Sarajevo - Bosnia and Herzegovina
12. Prof.Dr. Lada Lukić Bilela - University of Sarajevo - Bosnia and Herzegovina
13. Prof.Dr. Lukman Thalib - Qatar University - Qatar
14. Prof.Dr. M. Asghar Fazel - University of Environment - Iran
15. Prof.Dr. Mehmet Kitiş - Süleyman Demirel University - Turkey
16. Prof.Dr. Muhammad Arshad Javed - University of the Punjab Lahore - Pakistan
17. Prof.Dr. Muhammad Ovais OMER - University of Veterinary and Animal Sciences (UVAS)
18. Prof.Dr. Noureddine Djebli - Mostaganeml University - Algeria
19. Prof.Dr. Nuri Azbar - Ege University - Turkey
20. Prof.Dr. Özer Çınar - Yıldız Technical University - Turkey
21. Prof.Dr. Rifat Skrijelj - University of Sarajevo - Bosnia and Herzegovina
22. Prof.Dr. Samir Đug - University of Sarajevo - Bosnia and Herzegovina
23. Prof.Dr. Suad Bećirović - International University of Novi Pazar - Serbia
24. Prof.Dr. Tanju Karanfil - Clemson University - USA
25. Prof.Dr. Vladyslav Sukhenko - National University of Life and Environmental Sciences of Ukraine (Kyiv) - Ukrain
26. Assoc. Prof.Dr. Abdurrahman Akyol - Gebze Technical University - Turkey
27. Assoc. Prof.Dr. Alaa Al Hawari - Qatar University - Qatar
28. Assoc. Prof.Dr. Kateryna Syera - National University of Life and Environmental Sciences of Ukraine (Kyiv) - Ukraine
29. Assoc. Prof.Dr. Mostafa Jafari - Research Institute of Forests and Rangelands - Iran
30. Assoc. Prof.Dr. Nusret Drešković - University of Sarajevo - Bosnia and Herzegovina
31. Assoc. Prof.Dr. Yuriy Kravchenko - National University of Life and Environmental Sciences of Ukraine (Kyiv) - Ukraine
32. Assist. Prof.Dr. Ahmad Talebi - University of Environment - Iran
33. Assist. Prof.Dr. Ahmet Aygün - Bursa Technical University - Turkey
34. Assist. Prof.Dr. Mostafa Panahi - Islamic Azad University - Iran
35. Assist. Prof.Dr. Rishee K. Kalaria - Navsari Agricultural University - India
36. Assist. Prof.Dr. Sasan Rabieh - Shahid Beheshti University - Iran
37. Assist. Prof.Dr. Ševkija Okerić - University of Sarajevo - Bosnia and Herzegovina
38. Assist. Prof.Dr.Hasan Bora Usluer - Galatasaray University - Turkey
39. Assist. Prof.Dr. J. Amudhavel - VIT Bhopal University - India
40. Dr. Zsolt Hetesi - National University of Public Service, Budapest - Hungary
41. Dr. Zsolt T. Németh - National University of Public Service, Budapest - Hungary

ORGANIZATION COMMITTEE

Chairman(s) of the Conference

Prof. Dr. Özer Çınar – Yıldız Technical University

Members of the Committee

Prof. Dr. M. Asghar Fazel (Co-Chairman) – University of Environment

Dr. Gábor Baranyai (Co-Chairman) – National University of Public Service, Budapest

Prof. Dr. Samir Đug, University of Sarajevo

Assist. Prof. Dr. Sasan Rabieh Shahid Beheshti University

Assist. Prof. Dr. Ševkija Okerić - University of Sarajevo

Assist. Prof. Dr. Nusret Drešković - University of Sarajevo

Assist. Prof. Dr. Ranko Mirić - University of Sarejevo

Musa Kose - Zenith Group Sarajevo

Ismet Uzun - Zenith Group Sarajevo

Alma Ligata - Zenith Group Sarajevo

WELCOME TO ICOEST 2025

*On behalf of the organizing committee, we are pleased to announce that the **11th** International Conference on Environmental Science and Technology (**ICOEST-2025**) is held in **Sarajevo, Bosnia and Herzegovina on October 22-26, 2025.** ICOEST provides an ideal academic platform for researchers to present the latest research findings and describe emerging technologies, and directions in Environmental Science and Technology. The conference seeks to contribute to presenting novel research results in all aspects of Environmental Science and Technology. The conference aims to bring together leading academic scientists, researchers and research scholars to exchange and share their experiences and research results about all aspects of Environmental Science and Technology. It also provides the premier interdisciplinary forum for scientists, engineers, and practitioners to present their latest research results, ideas, developments, and applications in al lareas of Environmental Science and Technology. The conference will bring together leading academic scientists, researchers and scholars in the domain of interest from around the world. ICOEST is the oncoming event of the successful conference series focusing on Environmental Science and Technology. The scientific program focuses on current advances in th eresearch, production and use of Environmental Engineering and Sciences with particular focus on their role in maintaining academic level in Science and Technology and elevating the science level such as: Water and waste water treatment, sludge handling and management, Solid waste and management, Surface water quality monitoring, Noise pollution and control, Air pollution and control, Ecology and ecosystem management, Environmental data analysis and modeling, Environmental education, Environmental planning, management and policies for cities and regions, Green energy and sustainability, Water resources and river basin management. The conference's goals are to provide a scientific forum for all international prestige scholars around the world and enable the interactive exchange of state-of-the-art knowledge. The conference will focus on evidence-based benefits proven in environmental science and engineering experiments.*

Best regards,
Prof. Dr.Özer ÇINAR

ICOEST SARAJEVO
11TH INTERNATIONAL CONFERENCE ON ENVIRONMENTAL SCIENCE AND TECHNOLOGY
October 22-26 2025 I Sarajevo

ICOEST SARAJEVO
11TH INTERNATIONAL CONFERENCE ON ENVIRONMENTAL SCIENCE AND TECHNOLOGY
October 22-26 2025 I Sarajevo

Positive Effects of Developments in the IT Sector on the Commercial Relations And Environmental Activities of Maritime Businesses

Tayfun Acarer[1*]

[1]PIRI REIS UNIVERSITY

*tacarer@hotmail.com

Abstract:

The IT sector, where the impact of technological advancements is most pronounced, has been experiencing rapid and aggressive changes in recent years. This sector, which acts as a driving force for other sectors, is developing at a dizzying pace alongside technological advancements, and all sectors are significantly impacted by these developments.

The significant increase in speed and decreasing latency, particularly in internet and broadband data communication in recent years, has significantly positively impacted businesses' commercial relationships, access to information, and communication. As a result, the emergence of numerous digital evaluation elements today has led to significant changes in businesses' decision-making processes and business models.

The maritime sector is currently one of the areas where the impact of IT is most pronounced. Business conditions, competition, and applicable regulations dictate that businesses in this sector closely monitor technological developments in the IT sector and utilize these advancements to the fullest extent.

Today, shipping companies can easily communicate with ships using various maritime communication systems. This allows for easy monitoring of ship activities, meeting needs, monitoring malfunctions, and ensuring timely transfers of seafarers. Furthermore, these developments allow maritime businesses to electronically track the entire process, from cargo transfer to the ship, insurance, and handling at the port to delivery to the recipient. This significantly reduces delays in ship voyages, cargo spoilage, and potential penalties. With advancements in container technology and communication systems, tracking containers across countries can now only be achieved through smart systems and artificial intelligence.

One of the most significant reflections of the IT sector today is the "Blockchain" platform. Cryptocurrencies are considered the most important output of Blockchain. Cryptocurrencies are currently heavily used in both payment systems and cash flows by institutions. As a result, the use of cryptocurrencies is increasingly widespread in the maritime sector, where international relations are among the most intense and complex.

Today, most navigation and machinery systems on ships are operated remotely. Furthermore, sensors placed at various points throughout the ship allow for remote monitoring of system status and intervention when necessary. This capability has led to the emergence of land-based units within maritime operations that undertake the task of monitoring ships and troubleshooting specific malfunctions remotely.

Consequently, it is no longer a choice but a necessity for businesses in the maritime sector, one of the sectors most affected by technological advancements in information technology, to closely monitor these developments and reshape their operations accordingly. This is because it is virtually impossible for companies in this sector to continue operating without taking advantage of these advancements.

Keywords: Commercial Activities Of Maritime Businesses, Information Technology Sector, Maritime Communication, Broadband Data

ICOEST SARAJEVO
11TH INTERNATIONAL CONFERENCE ON ENVIRONMENTAL SCIENCE AND TECHNOLOGY
October 22-26 2025 I Sarajevo

Life Cycle Carbon Footprint of a 1 Mw Pv Plant in Bosnia And Herzegovina

Nurin Zecevic[1], Lejla Pajt[1], Azrudin Husika[1]*

[1]University Of Sarajevo

*zecevicn@mef.unsa.ba

Abstract:

Photovoltaic (PV) power plants are a key sustainable energy technology, but their environmental impact varies significantly across life cycle stages. This paper evaluates the carbon footprint of a 1 MW PV plant in Bosnia and Herzegovina (BiH) over a 25-year lifespan using Life Cycle Assessment (LCA) methodology (ISO 14040/14044). The analysis covers emissions from material production, installation, operation, and recycling. Results indicate that over the expected 25-year lifespan, the PV plant generates a total energy output of 31,036 MWh, accounting for a 1% annual power degradation rate due to efficiency losses. The highest emissions occur during material production (70–80% of total), while the operational phase offsets 20,173.5 tCO_2eq compared to BiH's grid emissions (0.65 tCO_2/MWh). The total CO_2 emission balance is highly dependent on the grid emission factor, which was assumed constant in this study. This factor is expected to decline due to the projected reduction in coal-based electricity generation. The net lifecycle emissions amount to -20,358.35 tCO_2eq, demonstrating PV's climate mitigation potential. The recycling phase assumes full material substitution, eliminating the need for new raw materials. However, the recycling process for all PV modules requires energy, estimated at 5,661 kWh, with a portion assumed to be supplied by renewables. Key recommendations include localizing PV component manufacturing to reduce transport emissions, optimizing logistics, developing recycling infrastructure, and increasing the share of renewable energy in manufacturing to further reduce emissions. This research provides a framework for sustainable PV systems in BiH, highlighting policy and technological pathways to enhance environmental performance. Future research should investigate advanced materials, recycling innovations, hybrid systems to maximize land-use efficiency, and region-specific energy payback periods to support BiH's energy transition.

Keywords: Photovoltaic Systems, Carbon Footprint, Life Cycle Assessment, Renewable Energy, Bosnia And Herzegovina

ICOEST SARAJEVO
11TH INTERNATIONAL CONFERENCE ON ENVIRONMENTAL SCIENCE AND TECHNOLOGY
October 22-26 2025 I Sarajevo

Physiological And Biochemical Responses of Raphanus Sativus Plants to Abiotic Stress

Flavia Bortes[1], Lucian Copolovici[1], Cristian Moisa[1], Andreea Lupitu[1], Dana Copolovici[1]*

[1]Aurel Vlaicu University of Arad

*flaviabortes@yahoo.com

Abstract:

Elevated temperatures and aridity adversely affect plant growth by inducing leaf curling, dehydration, the buildup of toxins and reactive oxygen species, and significant physiological disruption, ultimately leading to diminished yields. Enhancing thermotolerance and resilience in plants is crucial for guaranteeing food security. This can be achieved by breeding and agronomic approaches that leverage the inherent defenses of plants, including osmotic adjustment, heat-shock proteins, and antioxidant systems.

This study investigated the interactive effects of drought and acute heat stress on photosynthetic performance, pigment composition, and biochemical characteristics in plants of the Brassicaceae family, focusing on the genus Raphanus sativus L. var. "Johanna" and "Helga". To resolve order effects, a sequential stress model was used: (i) drought→heat (D→H) and (ii) heat→drought (H→D). In D→H, irrigation was interrupted for 3 days to induce a slight soil water deficit, after which the plants were subjected to a 5-minute heat pulse at 30, 40, 50, or 60 °C. In H→D, the same heat treatment preceded the 3-day drought period.

Photosynthetic parameters (net CO_2 uptake (A) and stomatal conductance to water vapor (g_sw)) were measured in control and stressed plants using an gas exchange system. Photosynthetic pigments (chlorophyll a, chlorophyll b, and zeaxanthin) were quantified by UHPLC–DAD (ultra-high-performance liquid chromatography with diode array detection). Regarding the total phenols, the total concentration of flavonoids present in the plants decreases drastically after a short period of heat stress.

Keywords: Drought Stress, Plant Photosynthesis, Heat Stress.

ICOEST SARAJEVO
11TH INTERNATIONAL CONFERENCE ON ENVIRONMENTAL SCIENCE AND TECHNOLOGY
October 22-26 2025 I Sarajevo

Impact of Abiotic Stress on Bioactive Compounds And Antioxidant Capacity in Galium And Helichrysum

Flavia Bortes[1*], Lucian Copolovici[1], Cristian Moisa[1], Andreea Lupitu[1], Dana Copolovici[1],Maria Cojocaru-Toma[2],Angelica Ohindovschi[2],Mihaela Nartea[2]

[1]Aurel Vlaicu University of Arad
[2]Nicolae Testemitanu State University of Medicine And Pharmacy of the Republic of Moldova

*flaviabortes@yahoo.com

Abstract:

Plants from the Galium and Helichrysum genera are appreciated for their pharmacological qualities and traditional therapeutic use. Under abiotic stress, they induce the formation of bioactive chemicals (polyphenols and flavonoids), which protect cells and help plants defend themselves.

This study seeks to understand how abiotic circumstances such as drought and ozone affect the biochemical properties of medicinal plants.

Mature leaves of each Galium and Helichrysum species were collected from the marker batch and treated with two different abiotic stresses. The total flavonoid and polyphenol content was determined using a spectrophotometric technique. The antioxidant activity of each extract was evaluated simultaneously using DPPH, ABTS, FRAP, and CUPRAC.

Moderate abiotic stress enhanced phenolic and flavonoid accumulations: total polyphenols increased by 30–60% compared to the control, particularly in water-stressed conditions, whereas severe stress decreased concentrations, indicating overcoming adaptive potential. Antioxidant capacity (measured using CUPRAC, DPPH, FRAP, and ABTS techniques) rose by 35-50%, with extracts from dehydrated plants attaining their peak values. Polyphenol concentrations were associated strongly with antioxidant capacity, while increases in flavonoid concentrations accounted for an additional 10-15% increase in antioxidant activity.

Moderate abiotic stress, such as drought and ozone fumigation, stimulates polyphenol and flavonoid synthesis in the Galium and Helichrysum genera, thereby increasing antioxidant activity. Severe stress reduces these levels beyond the plants' ability to adapt.

This work was supported by a grant from the Romanian National Authority for Scientific Research, CNCS – UEFISCDI, project number PN-IV-P8-8.3-ROMD-2023-0022.

Keywords: Total Phenolic Compounds, Flavonoids, Abiotic Stress

ICOEST SARAJEVO
11TH INTERNATIONAL CONFERENCE ON ENVIRONMENTAL SCIENCE AND TECHNOLOGY
October 22-26 2025 I Sarajevo

FULL-TEXT ARTICLES

ICOEST SARAJEVO
11TH INTERNATIONAL CONFERENCE ON ENVIRONMENTAL SCIENCE AND TECHNOLOGY
October 22-26 2025 I Sarajevo

Quantifying Black Carbon Emissions Using Non-Instrumental Methods: A Framework Applied to Coast Guard Fleet in the Philippines

Janine Tubera Guevarra[1,2,3], Kim Kyoungrean[1,2,]*

Abstract

Black carbon (BC) emissions originating from the maritime sector pose serious risks to both the global climate and human health. A short-lived climate pollutant that contributes to the melting of Arctic ice, influences weather patterns, and is associated with cardiopulmonary diseases. Despite its impact, several domestic fleets and those operated by the Philippine Coast Guard (PCG) lack real-time onboard monitoring capability for BC emission measurement. This disparity stresses the need to use alternative non-instrumental methods for accurate emission tracking, eventually leading to the development of effective mitigation strategies.

We develop a systematic framework for estimating BC emissions, using existing data and acknowledged guidelines, identifying the key high-emission activities, particularly berthing, which account for a large share of total emissions. We find that berthing contributes 70% of the sampled emissions, significantly more than the underway phase (27%) and the docking and undocking phases (3%). The total sampled emissions are 0.1707 metric tons, with 0.1203 metric tons from berthing alone. This research exhibits that non-instrumental approaches can reliably produce BC emission profiles in data-scarce settings, with the emphasis on the importance of prioritizing port-related emissions for effective policy implementation. The framework, based on EEA Guidelines coupled with ship details and activity profiling, offers a solid and repeatable method for establishing baseline emission inventories, assisting informed policy decisions, and sustainable maritime practices. This novel application of non-instrumental techniques to a real-world fleet without advanced monitoring shows its potential for broader use, offering a practical route reducing global BC emissions.

Keywords: black carbon, berthing emissions, framework, mitigation strategy, non-instrumental

1. INTRODUCTION

1.1. Black Carbon in Maritime: A Hidden Threat from Climate to Public Health

Maritime shipping is the key to support the global economy and trade, as it is the most cost-effective and energy-efficient means of transporting cargo over long distances. It contributes to economic resilience, most especially for island nations and countries where land-based transportation infrastructure is limited. Nevertheless, despite its critical importance, the sectors' environmental footprint has become a growing concern, particularly emissions like black carbon. Black Carbon (BC), one of the significant short–lived climate pollutants (SLCPs) and a component of fine particulate matter (PM 2.5), has been drawing global attention due to its warming effect in the atmosphere, which exceeds the impact of carbon dioxide (CO_2) [1], a known greenhouse gas. Emitted from the incomplete combustion of fossil fuels, biomass, and biofuels, BC absorb solar radiation, thereby contributing to atmospheric warming. It is later deposited on ice and snow, where it reduces albedo, thereby accelerating the melting process [2].

The maritime sector, a substantial contributor to anthropogenic BC emissions, accounts for more than 20% of carbon dioxide equivalent emissions over a 20-year timeframe, making it a significant climate-warming pollutant [3]. These emissions are particularly concerning because they are released directly into coastal and port areas, where they can severely degrade air quality and pose significant risks to public health and coastal marine resources.

Exposure to fine particulate matter, which includes BC, is associated with numerous serious health risks, including respiratory and cardiovascular diseases, premature death, and interferes with fetal development [4,5]. From a climate perspective, accelerated melting resulting from albedo reduction influences global climate patterns and hydrology [6], creating a positive feedback loop that further exacerbates global warming. Ecologically, when BC enters the marine

[1] Korea University of Science and Technology (UST), Korea (Republic of)
[2] Marine Environment Research Department, Korea Institute of Ocean Science and Technology (KIOST), Korea (Republic of), kyoungrean@kiost.ac.kr
[3] Philippine Coast Guard, Philippines (Republic of), ladyjaja2301@kiost.ac.kr
* Corresponding Author

ecosystem via dry deposition or river run-off, it has the potential to affect nutrient biogeochemical cycles, potentially impacting primary producers and broader food web functions [7, 8].

Although reducing BC emissions is widely recognized as necessary, the maritime sector confronts significant difficulties in tracking and controlling these pollutants. This difficulty arises as BC emissions are highly dependent and influenced by engine type and age, fuel quality, and operational modes [9]. Consequently, it makes the direct measurement and precise inventory compilation challenging, most especially for the older ships or vessels operating in areas with less strict environmental regulations. Many local fleets, particularly in developing countries, often lack the advanced sensors and real-time monitoring systems that the larger international shipping companies usually have. This technological disparity results in a substantial data gaps that hinder accurate emissions accounting and formulation of targeted mitigation strategies.

In the absence of onboard measurement capabilities, policymakers and researchers have to rely on estimated inventories, which are often limited by data availability and methodological consistency. As a result, the environmental impact of these fleets may be underreported, delaying much-needed regulatory attention and emissions reduction interventions [10].

1.2. Problem Statement

The absence of advanced onboard BC monitoring systems in various vessels, including military and law enforcement fleets such as those from the Philippine Coast Guard (PCG), presents a considerable challenge in managing emissions effectively. Without real-time data, the ability to start precise baseline emission inventories, identify high-emitting vessels or operational practices, and assess the effectiveness of ongoing mitigation strategies is limited. Conventional methods of emission estimation mostly rely on broad assumptions or require extensive instrumental measurements, which may not be practical and cost-effective for all maritime operators.

1.3. Policy Implications

This study has a significant implication for science and policy in maritime environmental protection. It demonstrates non-instrumental methods can effectively estimate black carbon (BC) emissions, providing an important tool for regions that lack the advanced monitoring capabilities. It democratizes emission assessment, allowing more stakeholders to contribute in reducing maritime pollution. The framework offers a model for establishing BC emission inventories, which will aid policy decisions, target setting, and progress tracking. Identifying berthing as the key BC source highlights strategies such as shore power and cleaner fuels, especially in improving air quality in the coastal communities. Additionally, the research supports using non-instrumental methods in scientific discourse on SLCPs, encouraging further investigation into BC emissions and refined models. Ultimately, it promotes sustainable maritime practices, environmental health, and climate change mitigation.

1.4. Research Objectives

1. Identify Non-Instrumental Methods: To explore and validate methodologies that utilize readily available data, such as ship profiles, fuel consumption, and emission factors, to estimate BC emissions from ships without direct instrumental measurements.

2. Establish Framework for PCG vessels' emission measurement: To develop a comprehensive measurement model for BC emissions based on established guidelines, specifically the European Environment Agency (EEA) Guidelines, integrated with detailed ship activity profiling.

3. Determine High-Emission Activities for focus-driven mitigation: To analyze the contribution of different operational phases—underway, docking, undocking, and berthing—to total BC emissions, thereby identifying activities that warrant prioritized mitigation efforts.

2. MATERIALS AND METHODS

2.1. Technical Overview of the Capital Vessels from the Coast Guard Fleet in the Philippines

The Philippine Coast Guard (PCG) is "established as an armed and uniformed service attached to the Department of Transportation" with provisions for attachment to the Department of National Defense during wartime [11]. It is vested with five functions: maritime safety, marine environmental protection, maritime security, maritime law enforcement, and search and rescue. It has twenty-seven (27) capital vessels, primarily used for implementing its five mandated functions. Multi-Role Response Vessel (MRRV), a 97-meter vessel used for patrolling within the Philippines' exclusive economic zone (EEZ), towing operations, maritime law enforcement, environmental protection, and humanitarian assistance and disaster response. Offshore Patrol Vessel (OPV), an 83-meter vessel used for extended offshore patrols in rough seas, pollution response, maritime domain awareness, multi-agency coordination, and environmental missions. Multi-Role Response Vessel (MRRV), a 44-meter vessel used for localized maritime law enforcement and security, search and rescue, environmental missions, logistical support, and aid in fisheries, immigration, and transnational crime enforcement. The Search and Rescue Vessel (SARV) is a 56-meter and 36-meter-sized vessel used for rapid response during search and rescue operations, coastal patrol and surveillance, and coastal environmental protection.

Although stipulated in the International Convention for the Prevention of Pollution from Ships, 1973 as modified by the Protocol of 1978 (MARPOL 73/78), Article 3 states, "shall not apply to any warship, naval auxiliary or other ship owned or operated by a State and used, for the time being, only on government non-commercial service, [12]." There is still a need to track and monitor its vessel emissions as it also explicitly states in Article 3 that "each Party shall ensure by the adoption of appropriate measures not impairing the operations or operational capabilities of such ships owned or operated by it, that such ships act in a manner consistent, so far as is reasonable and practicable, with the present Convention" [12]. As such, being the mandated organization to implement maritime environmental rules and regulations, it is necessary to track and monitor the PCG vessels' emissions to comply with Article 3 of the MARPOL 73/78 Convention.

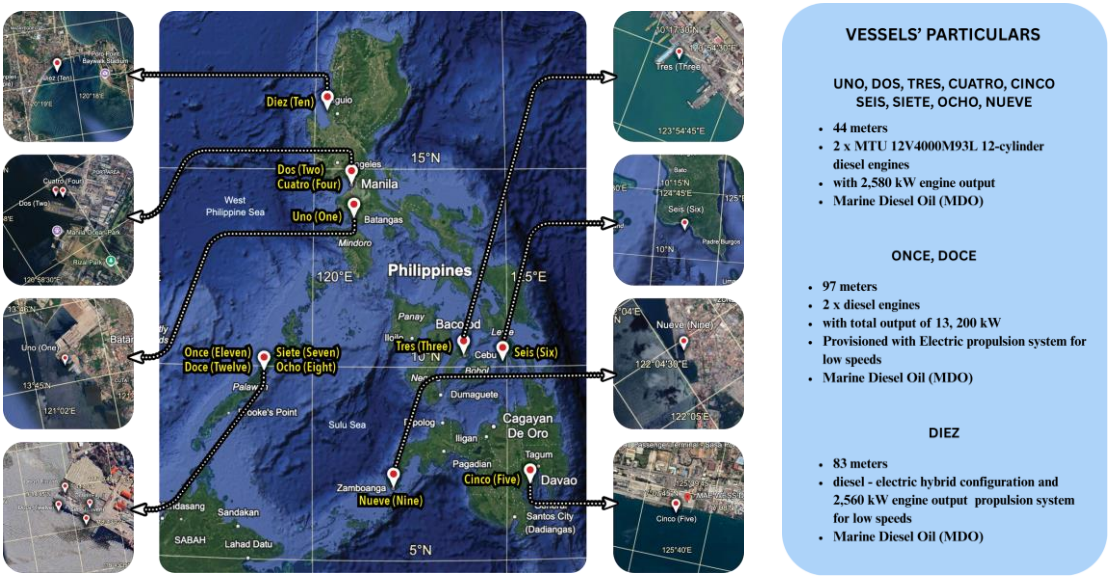

Figure 1. Overview of the PCG Vessels' Technical Specifications for Each Type (right)
Overview of the PCG Vessels' Operational Base Map in 2023 (left)

In this study, we utilized 12 of the 27 PCG's capital vessels, as they are the most frequently used and the largest, with the most recent complete data required for this study, while others have either incomplete data or are on dry dock. Vessels' technical specifications and location during the data collection are shown in Fig. 1.

2.2. Data Collection

This study conducted a comprehensive and detailed review of ship black carbon emissions, combining published literature and government records with estimation methods and reference to relevant environmental standards. We systematically search various journal databases such as ScienceDirect and Scopus for peer-reviewed articles and studies, and analyze reports from government and non-government organizations specializing in maritime environmental issues to ensure a broad, up-to-date understanding.

Moreover, we obtained the specific data of the vessels from the Philippine Coast Guard (PCG) official records, which include detailed ship specifications such as engine types, fuel consumption rates, and operational logs. These logs contain critical and most important data, as they reveal the ships' operational phases, including time spent underway, docking and undocking, and berthing, which is relatively crucial for implementing activity-based emission estimation methods.

2.3. Study Design

The study followed a structured approach to ensure systematic progression from the initial stages of problem identification to the final interpretation of results. A sequential context was adopted to guide each phase of the study, as shown in Fig. 2.

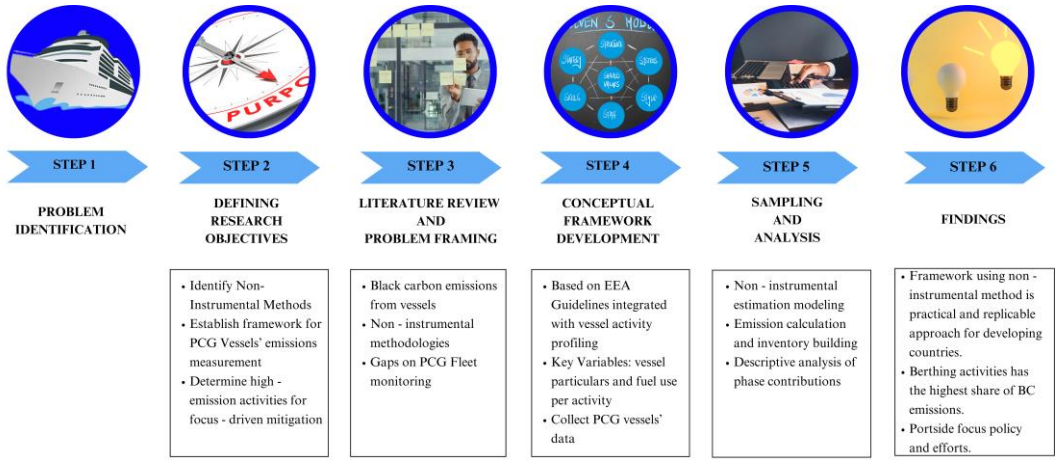

Figure 2. Methodological Flowchart: From Problem Definition to Key Findings

2.4. Non-Instrumental Methods

In the absence of direct instrumental measurements, black carbon emissions were estimated using the Tier III "Ship Movement Methodology" approach, consistent with established emission inventory guidelines of the European Environmental Agency [13]. This approach requires detailed ship movement data and technical information of the ship, such as engine size and technology, power installed or fuel use, and the duration of hours in different activities to quantify BC emissions. The formula used is:

$$E_{Trip,\,i,\,j,m} = \sum_{p}\left(FC_{j,\,m,\,p} \times EF_{i,\,j,\,m,\,p} \right) \quad (1)$$

Where:

E_{Trip} = emission over a complete trip (tonnes)

FC = fuel consumption (tonnes)

EF = emission factor (kg/tonne)

i = pollutant

m = fuel type

j = engine type

p = different phase of the trip (underway, docking/undocking, berthing)

2.5. Numerical Calculations

Since the data provided by the PCG only includes the total fuel consumption for the entire voyage duration, we assume docking and undocking durations of one hour (30 minutes each). This assumption aligns with their PCG Citizens Charter when responding to emergencies [14]. Additionally, we use a 15% load on the engine based on their set fuel consumption table. Similarly, for berthing, we consider a 100% load when using the auxiliary engine for the ship's power, according to its set fuel consumption table. Given the assumed values for berthing, we then calculated the fuel consumed in the auxiliary engine while underway and at berth using the data collected on the underway duration.

With the complete required data for calculation based on the EEA Tier III "Ship Movement Methodology," we were able to compute the black carbon emissions of the selected PCG Vessels.

2.6. Development of the Framework to Calculate Emissions from Vessels in the Philippines

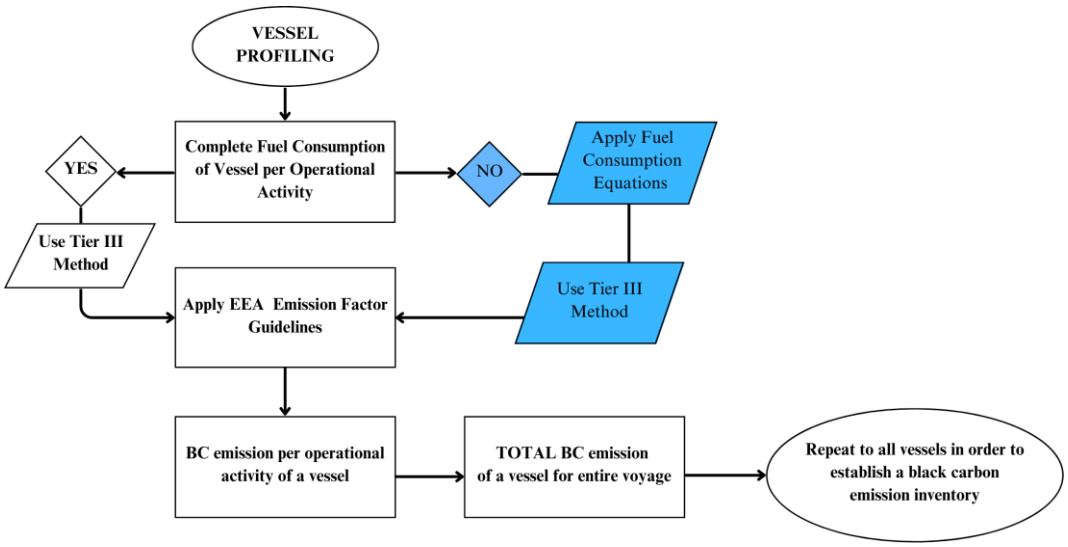

Figure 3. Preliminary Framework: Vessel-Level Emission Calculation Utilizing Non-Instrumental Methods

Based on the principles outlined in the EEA Emission Inventory Guidebook (2019) – Updated December 2021, integrated with detailed vessel profiling and activity-based analysis, a framework for estimating emissions from PCG vessels was developed, see Fig. 3. It can be visualized as a systematic process:

1. Vessel Profiling: The initial step of the framework involves gathering required data on each vessel, including its engine type, power output, specific fuel consumption (SFC), and fuel types used. This information is essential to apply the technology-specific emission factors in Tier III calculations.
2. Operational Activity (Fuel Consumption): Data on the operational activities of the vessels shall be collected from the vessels' activity logs and or automatic identification system (AIS). This includes the duration and fuel consumption during the three operational phases: underway (open sea transit), docking and undocking (navigating in confined waters, approaching/departing ports), and berthing (at berth, auxiliary engines running). In such cases where direct fuel consumption data for specific operational phases were unavailable, fuel consumption modeling equations shall be used to calculate these values.
3. Emission Factor Application: Emission factors for black carbon were primarily sourced from the EEA Emission Inventory Guidebook (2019) – updated 2021. These factors, which quantify the amount of pollutant emitted per unit of fuel consumed or activity performed, were applied according to the chosen tier of analysis. The framework allows for the application of Tier I (Default Approach), Tier II (Technology-Specific Approach), or Tier III (Ship Movement Methodology) based on the availability and granularity of data in possession.
4. Total BC Emissions per Operational Phase: By combining the fuel consumption data for each operational phase with the appropriate emission factors, the total black carbon emissions for each phase were calculated. This step was crucial for determining which operational activities contributed most significantly to the overall BC emissions.
5. Baseline Measurement**:** By integrating the results from the three operational phases—underway, docking/undocking, and berthing—the total black carbon (BC) emissions for each vessel were calculated. This comprehensive approach allowed for the establishment of a baseline measurement, providing a foundational reference point for assessing emission levels, tracking trends over time, and informing future mitigation strategies tailored to vessel behavior and port operations.

This systematic framework guaranteed a vigorous and transparent methodology to estimate not only black carbon emissions from PCG vessels but also other SLCPs, offering a reliable baseline for future mitigation efforts and policy development. The integration of literature review, government records, and established emission guidelines allowed for a comprehensive assessment even in the absence of direct instrumental measurements.

2.7. Statistical Analysis

Descriptive statistical analysis was employed to summarize and interpret the black carbon (BC) emissions data across the three operational phases of sampled vessels. Measures including percentages, totals, and distribution patterns were used to identify which phase contributed most significantly to overall emissions. The use of descriptive statistics effectively captured the emission behavior of vessels and provided a clear picture of where mitigation efforts should be prioritized.

3. RESULTS

3.1. Overview of Year 2023 PCG Vessels' Black Carbon Emission Results

Our analysis of black carbon (BC) emissions from the sampled Philippine Coast Guard (PCG) vessels in 2023 revealed a total emission of 0.1797 metric tons. This figure provides a foundational baseline for understanding the BC contribution from the observed fleet. A detailed breakdown of emissions per vessel indicated significant variability in its contributions. Specifically, Vessel Once (Eleven) exhibited the highest BC emissions at 0.0292 metric tons, likely due to its significantly larger size of 97 meters, allowing for greater engine power and fuel use, also suggesting potential differences in operational profiles, engine efficiency, or fuel consumption practices that may warrant further study. In contrast, other vessels contributed lower but still considerable emission levels. Therefore, it implies that vessel size, in combination with operational patterns and engine specifications, plays a critical role in determining BC emissions. Given that the individual emissions may appear modest, the cumulative impact from such vessels, especially when considered fleet-wide and over time, underscores the importance of targeted emission reduction strategies.

Table 1. The amount of PCG vessels' black carbon emissions in 2023

Vessel Name	Underway	Docking/Undocking	Berthing	TOTAL	TOTAL
	(kg)	(kg)	(kg)	(kg)	(ton)
Doce (Twelve)	9.379	0.6169	18.32	28.32	0.0283
Once (Eleven)	9.880	0.1707	19.16	29.21	0.0292
Diez (Ten)	4.190	0.1607	19.04	23.39	0.0234
Nueve (Nine)	2.616	0.5370	7.511	10.66	0.0106
Ocho (Eight)	2.234	0.6006	5.908	8.743	0.0087
Siete (Seven)	4.697	0.4627	6.919	12.08	0.0121
Seis (Six)	1.935	0.3470	7.714	10.00	0.0100
Cinco (Five)	1.020	0.1157	5.958	7.094	0.0071
Cuatro (Four)	4.903	0.5783	6.875	12.35	0.0123
Tres (Three)	1.333	0.2313	7.567	9.042	0.0090
Dos (Two)	1.271	0.1349	7.532	8.876	0.0089
Uno (One)	2.572	0.7133	7.829	11.11	0.0111

3.2 Emission Concentrations by Operational Activities

One of the most substantial findings of this study is the disproportionate contribution of different operational activities to the total black carbon emissions. The analysis demonstrated that berthing (vessels at berth with auxiliary engines running) accounted for the largest share of BC emissions, contributing approximately 70% of the total sampled emissions or 0.1203 metric tons of BC.

Whereas, the underway phase (open sea transit) contributed 27% of the emissions, and the docking/undocking phase was responsible for about 3%.

This distribution emphasizes the indispensable insight that the majority of BC emissions occur when vessels are stationary or operating at low speeds within or near port areas. This finding is particularly relevant for air quality and warming potential within coastal cities and port communities, as these emissions are released in close proximity to human populations. The representation as shown in Table 2 illustrates the dominance of berthing emissions, providing compelling evidence for focus-driven mitigation efforts that target reducing emissions during port stays.

Table 2. Distribution of Black Carbon Emissions by Operational Phase of Vessels

Underway	Docking/Undocking	Berthing	TOTAL	TOTAL
(kg)	(kg)	(kg)	(kg)	(ton)
46.03	4.669	120.3	170.9	0.1707

3.3 Key Findings and Observations

Based on the quantitative results and qualitative observations, several key findings emerged:

1. Port Areas as Emission Hotspots: Berthing activities appeared as the dominant trace of BC emissions, thus emphasizing that critical emission hotspots are in port areas. Prolonged running of vessels' auxiliary engines while berthed leads to concentrated pollution, intensifying health risks to port workers, users, and nearby communities.
2. Health and Climate Risks: High concentrations of BC emissions in ports pose severe health threats, such as cardiopulmonary diseases, regional warming impact, and coastal environmental degradation. These findings accentuate the urgent need for mitigation schemes in high-exposure zones.
3. Methodological Validation and Limitations: The study validates the practicality of non-instrumental methods to estimate BC emissions in instances where direct monitoring is unavailable. However, though the approach based on EEA guidelines and vessel activity profiling is practical and efficient for baseline inventories, it has limitations due to reliance on data reported and a lack of real-time validation. Still, it offers a valuable, accessible tool for policy development and initial assessments.

These results show a clear outline of the black carbon emission footprint within the sampled PCG fleet, emphasizing the contribution of berthing activities and underscoring the need for targeted interventions to achieve sustainable mitigation. The findings laid the groundwork for the subsequent discussion on implications and policy recommendations.

4. DISCUSSIONS

The outcome, indicating that berthing activities account for the majority proportion of the total black carbon emissions from PCG vessels, conveys significant implications for environmental policy and operational practices. This disparity contribution outlines that the most impactful mitigation efforts should be directed towards vessels while they are berthed in ports. Berthing explicitly involves ships running auxiliary engines to power onboard systems, lighting, and crew needs, often for extended periods. Unlike underway or docking/undocking, which occur over wider geographical areas, berthing emissions are concentrated in confined port environments, directly influencing the air quality of adjacent urban areas, the health of port workers and residents, as well as nutrient cycles in the coastal marine ecosystem.

This emission concentration generates localized pollution hotspots, worsening cardiopulmonary health issues for communities near ports. The environmental impact extends beyond human health, contributing to regional haze and localized warming effects. Therefore, addressing berthing emissions is not only an environmental necessity but also a public health priority.

5. CONCLUSIONS

This study stresses the potential of non-instrumental methods to estimate black carbon (BC) emissions from ships, most especially when onboard monitoring systems are unavailable. Utilizing the Philippine Coast Guard fleet as a model, it established a reliable framework aligned with EEA guidelines. Berthing activities contribute the highest share of BC emissions, thus underscoring the need for targeted portside policies like electrification and cleaner fuels. The research provides a practical, replicable approach for developing countries, offering both a baseline inventory and a scalable method to support global efforts towards sustainable maritime operations.

ACKNOWLEDGMENT

This research was supported by Korea Institute of Ocean Science and Technology (PO01458), Korea (Republic of).

REFERENCES

[1] Climate and Clean Air Coalition. (n.d.). Black carbon. United Nations Environment Programme. Retrieved January 28, 2025, from https://www.ccacoalition.org/short-lived-climate-pollutants/black-carbon
[2] Clarity Movement. (2025, April 12). Albedo reduction caused by black carbon. Clarity Movement. [Online]. https://www.clarity.io/blog/albedo-reduction-caused-by-black-carbon
[3] International Council on Clean Transportation. (2019). Black carbon from shipping accounts for more than 20% of CO_2-equivalent emissions over 20 years. ICCT Policy Update.
[4] World Health Organization. (2021). Health effects of black carbon. WHO Regional Office for Europe.
[5] Johnson, B. R. et al. (2021). Air pollution and children's health: a review of adverse effects associated with prenatal exposure from fine to ultrafine particulate matter. Environmental Health and Preventive Medicine, 26(1), 1–12. (summary review)
[6] Rutherford, W. A. et al. (2017). Albedo feedbacks to future climate via climate change impacts on dryland biocrusts. Scientific Reports, 7, 44188. https://doi.org/10.1038/srep44188
[7] Mari, X., Guinot, B., Thuoc, C. V., Brune, J., Lefebvre, J. P., Angia Sriram, P. R., ... & Niggemann, J. (2019). Biogeochemical impacts of a black carbon wet deposition event in Halong Bay, Vietnam. Frontiers in Marine Science, 6, 185.
[8] Saidi, A., Zoccarato, L., Birarda, G., Mari, X., Weinbauer, M., Vaccari, L., ... & Malfatti, F. (2025). Black carbon structuring marine microbial activities and interactions: a micro-to macro-scale interrogation. Environmental Science and Pollution Research, 1-19.
[9] Le Berre, L., Temime-Roussel, B., Lanzafame, G. M.,D'Anna, B.,Marchand, N.,Sauvage, S.,Wortham, H. (2025).

[10] Measurement report: In-depth characterization of ship emissions during operations in a Mediterranean port. Atmospheric Chemistry and Physics, 25, 6575–6605. https://doi.org/10.5194/acp-25-6575-2025
[11] Dettner, F., & Hilpert, S. (2022). Emission inventory for maritime shipping emissions in the North and Baltic Sea (2015). arXiv preprint arXiv:2211.13129.
[12] Republic of the Philippines. (2010, February 12). Republic Act No. 9993: Philippine Coast Guard Law of 2009.
[13] International Convention for the Prevention of Pollution from Ships, 1973, as amended by the Protocol of 1978 (MARPOL 73/78), art. 3(3), 1340 U.N.T.S. 22484 (entered into force Oct. 2, 1983).
[14] European Environment Agency. (2021). EMEP/EEA air pollutant emission inventory guidebook 2019: Updated December 2021 – Technical guidance to prepare national emission inventories. Publications Office of the European Union. https://www.eea.europa.eu/publications/emep-eea-guidebook-2019
[15] Philippine Coast Guard. (2024). PCG Citizens' Charter. Retrieved May 8, 2025, from https://www.coastguard.gov.ph

BIOGRAPHY

Janine Tubera Guevarra is a Philippine Coast Guard officer currently pursuing a Master's degree at the Korea Institute of Ocean Science and Technology (KIOST) under the London Protocol Engineering Master of Project Administration program. Her current research focuses on developing cost-effective and sustainable methods to calculate black carbon emissions, aiming to identify targeted solutions that will support compliance with the Paris Agreement. Looking ahead, she plans to establish a baseline inventory of black carbon emissions from domestic fleets in the Philippines, laying the groundwork for future mitigation strategies. Ultimately, her work aspires to inform policy development that mitigates global warming and helps lower temperatures in alignment with international climate goals.

ICOEST SARAJEVO
11TH INTERNATIONAL CONFERENCE ON ENVIRONMENTAL SCIENCE AND TECHNOLOGY
October 22-26 2025 I Sarajevo

Bio-Heat Transfer In Cancer Treatment Using Radiotherapy And Hyperthermia: "A General Mathematical Solution Of Pennes' Bio-Heat Equation Using Monte Carlo Simulation"

Tuka Fattal [3], Recep Yumrutaş [4]*

Abstract

This study presents a focused investigation of bio-heat transfer during radiotherapy enhanced by hyperthermia, aiming to optimize cancer treatment outcomes by maximizing tumor destruction while minimizing toxicity to surrounding healthy tissues. A thorough understanding of thermal dynamics during therapy enables clinicians to enhance treatment efficacy, predict biological responses based on dose parameters, and reduce adverse effects. Specifically, this work examines the synergistic combination of hyperthermia and X-ray radiotherapy. During the relaxation intervals between hyperthermia pulses—when the biological system responds to elevated temperatures (43 °C, 45 °C, 47 °C)—a radiation dose is administered. The underlying hypothesis is that heating tumor tissue increases its radiosensitivity, potentially reducing treatment time and improving therapeutic outcomes. A review of current literature supports this synergistic effect, showing that elevated temperatures intensify cellular damage. The Arrhenius damage model was employed to quantify this relationship, translating temperature and exposure duration into a single thermal damage parameter (Ω) representing irreversible tissue injury. A general mathematical framework for simulating this process was developed using Monte Carlo photon transport to generate spatially distributed heat sources, and Pennes' bio-heat equation was solved to model heat transfer within layered biological tissue.

Keywords: Bio-heat transfer, Cancer treatment, Hyperthermia, radiotherapy, Pennes' bio-heat equation, Monte Carlo Simulation.

1. INTRODUCTION

Radiation therapy is one of the most common cancer treatment methods[1]**,** Radiotherapy started to be used by the 20thcenturay after Mari Cori discovered radiation where ionizing irradiation started to be used to shrink tumor size. Radiotherapy can be applied alone or in corporation with other therapy methods such as chemotherapy, or surgery [2]**,** [3]**.** The needed exact dose of the radiotherapy is the main concern and the foremost goal of radiotherapy, as it should be strong enough to eliminate the tumor and not cause much harm of the aligned tissues or organ and this is the main dilemma. Radiotherapy center must be in any cancer curing plans of any government for simple reasons as the radiotherapy help in the early detection of the diseases [4]**.** During cancer treatment process we have to consider the volume of the coagulation zone the area that would not be able to recover after exposing to radiation including the tumor cells [5]**,** predicting the size of this area is crucial as we want to minimize the negative impact of radiation on the normal tissues and allow it to recover after finalizing the treatment. On the other hand, a good treatment plan aims to ensure the full destruction of the tumor in an irreversible way, minimizing radiation therapy known side effects allows to safe the surrounding healthy tissues such as adjacent organs, nerves, and blood vessels and destroying the tumor entirely is the main objective of a good treatment plan [5]**,** [6]**.** Hyperthermia considered as one of the used types to treat cancer. Using hyperthermia as a treatment method started in the 19thcentury W.B. Coley succeed decreasing his patient tumor size [7]**.** Where cancer cells are exposed to high temperature (up to 44-45 C̊) approximately for one hour [8]**.** Based on clinical experiments and researches high temperature the heat used to localize and by concentrated heating sources, cancer cells can be destroyed. Working mechanism is destroying the proteins and the structure within cancer cells, its lead to shrink tumor's volume with minimum side effects to normal tissues. Hyperthermia/HT significantly affects the microenvironment, immune responses, vascularization, and oxygen supply of tumors. Clinical trials showed that using hyperthermia was not toxic to normal cells while inducing toxicity in cancerous cells [9]**.** The combination between Radiotherapy and Hyperthermia methods started specifically in 1970s where thermos-radiotherapy (TRT) has been demonstarted to enhance cancer treatment outcomes, when its compared

[3] Corresponding author: Gaziantep University, Department of Mechanical Engineering-Energy Division, 27410 Şahinbey/Gaziantep, Türkiye. drtukafattal78@gmail.com
[4] Gaziantep University, yumurtas@gantep.edu.tr

to Radiotherapy alone, without increasing serious undesirable side effects, at least for several advanced cancers, such as breast, cervical, esophageal, lung, head and neck.

2. MATERIALS AND METHODS

In this study, we explored a hybrid treatment strategy that combines laser-induced hyperthermia with X-ray radiotherapy to enhance cancer cell destruction while protecting surrounding healthy tissue. A synthetic 3D lung-tumor model was developed to simulate this approach, using advanced computational tools to mimic realistic treatment conditions. We began by applying a laser-based external heat source to raise the tumor temperature in controlled phases—specifically to 43 °C, 45 °C, and 47 °C. For each temperature phase, we calculated the 3D distribution of energy deposition within the tissue using Monte Carlo photon transport simulations (MCXLAB) [10]**.** These results were used to define a spatially varying heat source term, which was then incorporated into the Pennes' bio-heat transfer equation to predict how the tumor temperature evolves over time. To assess the biological impact of heating, we used the Arrhenius thermal damage model to estimate the extent of irreversible damage caused to cancer cells. After each heating phase, we simulated the application of X-ray radiation during the relaxation period, modeling the X-ray dose distribution using Monte Carlo methods and estimating its biological effectiveness using the Linear-Quadratic (LQ) model [11]**.** for cell survival. Finally, we compared all three heating phases—43 °C, 45 °C, and 47 °C—based on thermal damage levels and radiotherapy outcomes. This allowed us to evaluate which temperature best balances effective tumor damage with minimal harm to healthy tissue, helping inform future treatment planning for hyperthermia-assisted radiotherapy. To model heat transfer during tumor hyperthermia, a simplified spherical control volume was constructed, consisting of a central tumor region surrounded by concentric layers of healthy lung tissue. The geometry assumes radial symmetry and allows the temperature distribution to be described in spherical coordinates. Blood perfusion was considered throughout the domain, and a convective heat loss boundary condition was applied at the outer surface to simulate thermal exchange with surrounding tissue or air. At the tumor center (r = 0), a symmetry condition was applied to ensure physical realism. This configuration provided a tractable yet physiologically relevant basis for solving Pennes' bio-heat equation under different thermal treatment scenarios. The figure illustrates the spherical control volume used to numerically solve Pennes' bio-heat equation for thermal modeling during hyperthermia treatment. The domain consists of a central spherical tumor surrounded by concentric healthy lung tissue.

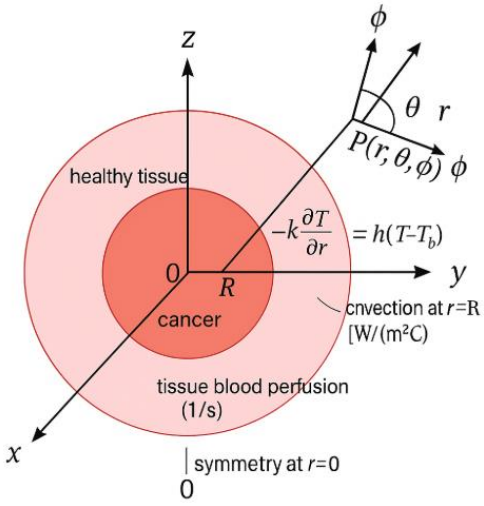

Figure 1 Spherical Tumor-Embedded Control Volume for Bio-Heat Transfer Analysis

This idealized geometry allows the use of spherical coordinates (r, θ, ϕ), which are well-suited for capturing the radial symmetry of heat diffusion and laser energy deposition. The tumor lies at the center (r = 0), where a symmetry boundary condition ensures no heat flux. At the outer radius (r=R), convective heat loss to surrounding tissues is modeled using a heat transfer boundary condition. Internal heat generation includes metabolic heat, blood perfusion effects, and an external laser source modeled from the Monte Carlo photon transport simulations. This control volume provides the physical basis for applying the time-dependent form of Pennes' equation [12]and predicting temperature rise and thermal damage throughout the tumor and adjacent tissue under different heating conditions (43 °C, 45 °C, and 47 °C phases). Before initiating hyperthermia, we developed a radially symmetric control volume that accurately mimics the anatomical layout of a solid tumor within surrounding healthy tissue. This voxel-based phantom, shown in the figure, provides an idealized yet realistic foundation for simulating bioheat transfer. The spherical symmetry of the model allows the Pennes' bio-heat equation to be applied in spherical coordinates, reducing numerical artifacts at boundaries and ensuring that heat gradients propagate

smoothly from the tumor core outward [13]. Additionally, the modular design of the phantom enables easy assignment of labels to represent distinct tissue layers (e.g., tumor, fat, muscle, skin), which becomes critical in later stages of layered thermal and radiative modeling. Based on the governing equation (Equation 1), and using the initial and boundary conditions, the Pennes' bio-heat transfer equation in spherical coordinates was solved numerically via an explicit finite difference method.

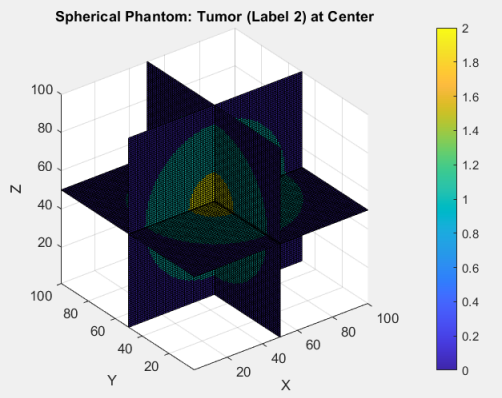

Figure 2 Voxelized 3D Spherical Phantom with Central Tumor (Label 2) and Surrounding Healthy Tissue (Label 1).

$$\rho c\ \frac{\partial T(r,t)}{\partial t} = \frac{1}{r^2}\frac{\partial}{\partial r}\left(r^2 K \frac{T(r,t)}{\partial r}\right) + \rho_b C_b\ \omega_b\left(T_a - T(r,t)\right) + Q_{met} + Q_{laser(r)} \qquad (1)$$

his method discretizes the equation in both time and space to simulate the transient temperature distribution within tissue subjected to laser heating and perfusion. The finite difference scheme was applied as follows:

- Time derivative (forward difference):
  $\frac{\partial T}{\partial t} \approx \frac{T_i^{n+1} - T_i^n}{\Delta t}$ (2)
- Spatial derivative in spherical form (central difference):

$$\frac{1}{\mathrm{r}^2}\frac{\partial}{\partial \mathrm{r}}\left(\mathrm{r}^2\frac{\partial \mathrm{T}}{\partial \mathrm{r}}\right) \approx \frac{1}{\mathrm{r}_\mathrm{i}^2}\left[\frac{\mathrm{r}_{\mathrm{i}+0.5}^2(\mathrm{T}_{\mathrm{i}+1}^\mathrm{n} - \mathrm{T}_\mathrm{i}^\mathrm{n}) - \mathrm{r}_{\mathrm{i}-0.5}^2(\mathrm{T}_\mathrm{i}^\mathrm{n} - \mathrm{T}_{\mathrm{i}-1}^\mathrm{n})}{\Delta \mathrm{r}^2}\right] \qquad (3)$$

Substituting these approximations into the original Pennes' equation, which includes heat conduction, perfusion, metabolic heat generation, and laser-induced heat input, yields the following update equation for temperature at each voxel and time step.

$$T_i^{n+1} = T_i^n + \frac{\Delta t}{\rho c}\left[\frac{k}{r_i^2}\left(\frac{r_{i+0.5}^2(T_{i+1}^n - T_i^n) - r_{i-0.5}^2(T_i^n - T_{i-1}^n)}{\Delta r^2}\right) + \rho_b c_b \omega_b (T_a - T_i^n) + Q_{met} + Q_{laser,i}\right] \qquad (4)$$

This scheme was implemented in MATLAB, where each voxel's temperature was iteratively updated over time until the desired preheating condition (43 °C, 45 °C, or 47 °C) was reached. The laser source was modeled as a Gaussian radial function, contributing to the $Q_{laser}(r)$ term, and representing spatially focused energy input. Meanwhile, metabolic heat generation Q_{met} was treated as a constant physiological parameter. The finite difference implementation enabled the tracking of spatial and temporal temperature dynamics critical to predicting thermal damage and guiding subsequent radiotherapy simulation.

3. RESULTS AND DISCUSSION:

3.1. First phase: Heating Tumor Tissue to 43°C

In the first hyperthermia phase, the central tumor region was heated to 43 °C using an external laser heat source. To model the light propagation within tissue, we employed MCXLAB, which simulated photon transport in the anatomically layered 3D phantom. The resulting fluence distribution was converted into a spatially resolved heat source term, $Q_{laser}(r)$, and incorporated into the time-dependent form of the Pennes' bio-heat transfer equation in spherical coordinates, as shown in equation 1. The simulation confirmed that the tumor core successfully reached 43 °C after approximately 900 seconds (15 minutes) of continuous laser exposure. Figure 3 shows a 3D overlay of the heated tumor region, highlighting the region that achieved the target temperature.

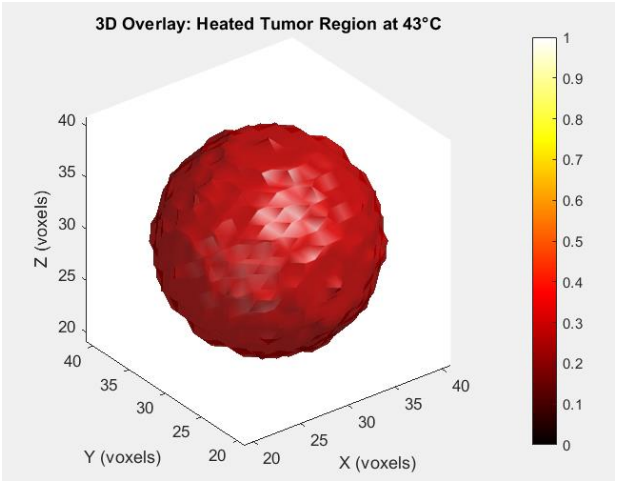

Figure 3 3D Overlay: Heated Tumor Region at 43°C

Estimating Thermal Damage: To evaluate the biological impact of heating the tumor to 43 °C, the Arrhenius thermal damage model was employed. This model is widely accepted for quantifying irreversible molecular injury caused by temperature elevation in biological tissues. It estimates the damage index, Ω(t), which reflects the logarithmic ratio of healthy to surviving molecules over time, and is sensitive to both temperature and exposure duration. The model uses the following integral expression:

$$\Omega(t) = \int_0^t A.\exp\left(-\frac{E_a}{RT(\tau)}\right)d\tau \qquad (5)$$

Where:

- Ω(t): Accumulated thermal damage index (unitless)
- A: Frequency factor (s^{-1}), representing molecular reaction rate
- E_a : Activation energy (J/mol), specific to tissue type
- R: Universal gas constant (8.314 J/mol·K)
- T(τ): Absolute temperature (in Kelvin) as a function of time

Ω: Dimensionless damage index (Ω ≥ 1 means irreversible damage)

A	3.1×10^{98} S^{-1}
E_a	6.28×10^{5} J/mol
R	8.314 J/mol. K
T	43+273.15=316.15K

Using the temperature-time profiles obtained from solving the Pennes' bio-heat equation, the Arrhenius thermal damage integral was numerically evaluated across the tumor and surrounding tissues. The results, shown in Figure 5, indicate that thermal damage values reached Ω ≈ 0.005 in the tumor center, reflecting sub-lethal injury, consistent with the goal of sensitizing cancer cells to subsequent radiotherapy without inducing irreversible ablation. Peripheral layers exhibited even lower damage values, further confirming the spatial selectivity of laser-based hyperthermia.

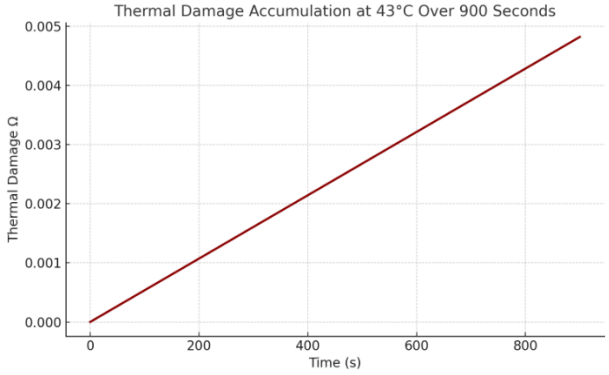

Figure 4 Thermal Damage Accumulation At 43 ℃ over 900 seconds.

X-ray Application During Relaxation (Post-Heating Phase 1): After elevating the tumor temperature to 43 °C via external laser-based hyperthermia, a targeted radiotherapy step was implemented. Specifically, a 6 MeV collimated X-ray beam was applied during the 5-minute (300 s) thermal relaxation period. This timing was strategically chosen to exploit the radiosensitizer state of tumor cells post-hyperthermia, thereby maximizing therapeutic efficacy while sparing surrounding healthy tissues. Monte Carlo simulations using MCXLAB were conducted to model photon transport and calculate the 3D spatial dose deposition. As visualized in Figure 6, the dose was concentrated at the tumor core with a Gaussian falloff, ensuring precision in tumor targeting while minimizing peripheral exposure.

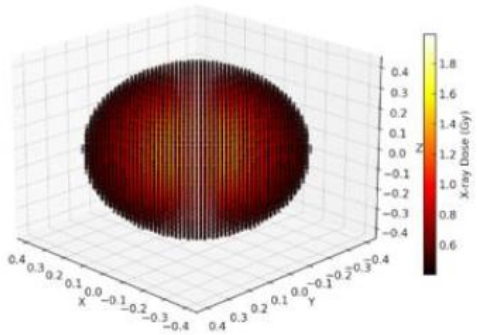

Figure 5 3D Spatial Distribution of X-ray Dose, following Laser-Induced Hyperthermia at 43 °C.

Combined Damage Assessment (Thermal + X-ray): To evaluate the cumulative effect of sequential hyperthermia and radiotherapy, we calculated the effective damage (ED) — representing the predicted fraction of cell death based on the combined thermal and radiative stresses. This model accounts for both the Arrhenius-based thermal injury and the dose-response to X-rays, highlighting their synergistic potential. Figure 7 shows the 3D volume rendering of the resulting cell death fraction, where each voxel represents the probability of irreversible damage. The central tumor region exhibits the highest values (ED ≈ 0.9), confirming that the combined treatment significantly enhances lethality compared to hyperthermia alone. As damage decreases toward the periphery, it also validates the selective targeting of the tumor core while sparing surrounding tissues. This volumetric result reinforces the core hypothesis of this study — that moderate hyperthermia (43°C) can sensitize tumor cells to radiation, leading to improved treatment efficacy without increasing radiation dose or thermal exposure beyond safe thresholds.

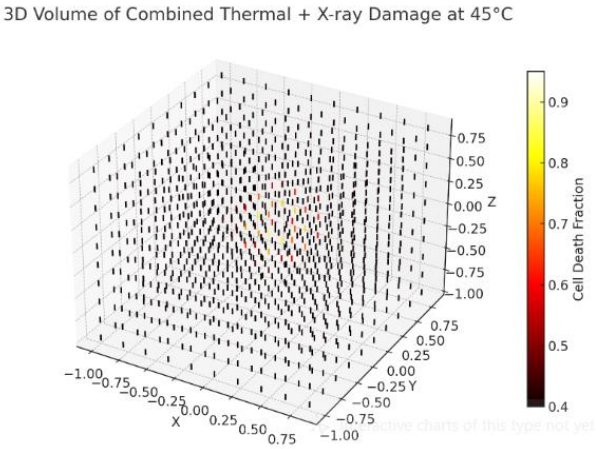

Figure 6 Visualization of Effective Cell Death Distribution After Combined Hyperthermia (43 °C) and X-ray Therapy.

A survival analysis conducted and its clearly demonstrates the selective lethality of the combined treatment approach. The tumor, heated to 43 °C and then exposed to 5 Gy X-rays, shows a dramatic drop in survival — only 6% of cells remain viable. In contrast, healthy tissue, which received a much lower dose (1.6 Gy) due to spatial attenuation, retained 71% survival, highlighting that normal structures were largely preserved. This result strongly supports the idea that moderate hyperthermia sensitizes tumor cells to radiotherapy, enhancing therapeutic efficacy without increasing the physical radiation dose — a key advantage in clinical settings where minimizing healthy tissue damage is crucial. As figure 8 demonstrates the survival analysis for both of tumor and health cells

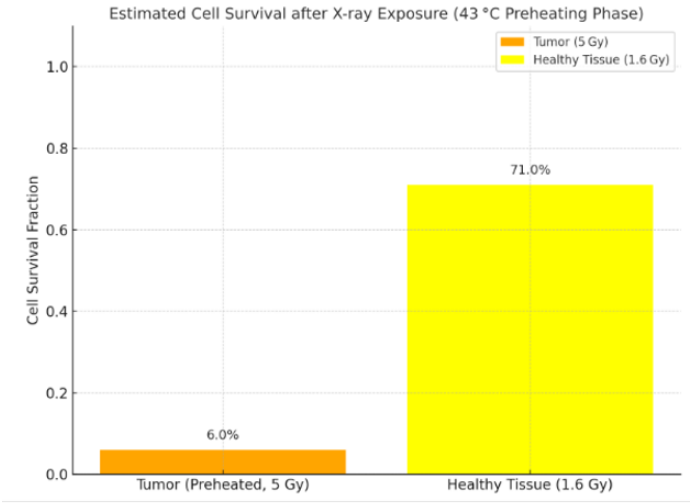

Figure7 Cell Survival Comparison Following 43 °C Hyperthermia and Radiotherapy (First Treatment Phase).

Second phase: Heating Tumor Tissue to 45°C: To ensure a comprehensive comparison and evaluate the impact of higher thermal exposure on treatment outcomes, all simulation steps conducted in the first heating phase (at 43 °C) were systematically repeated for a second phase, this time targeting a tumor temperature of 45 °C.

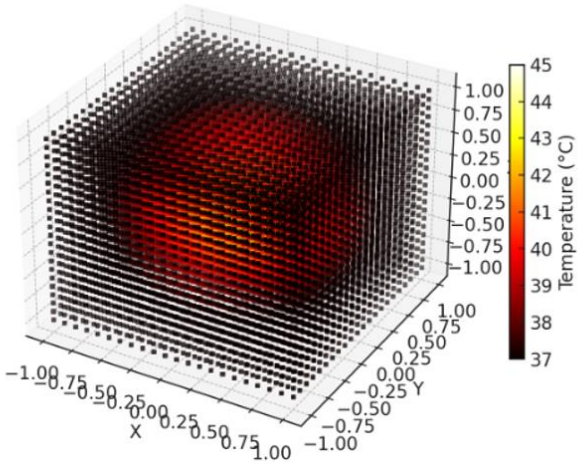

Figure 8 3D Cutaway View: Heat Distribution in Tumor and Tissues at 45 °C

Estimating Thermal Damage: During the second heating phase, the tumor was reheated from 37 °C to 45 °C using laser-based hyperthermia. Thermal damage estimation via the Arrhenius mode**.** At this temperature, the Arrhenius thermal damage index reached approximately $\Omega \approx 0.03$, which is about three times the damage observed at 43 °C ($\Omega \approx 0.005$).

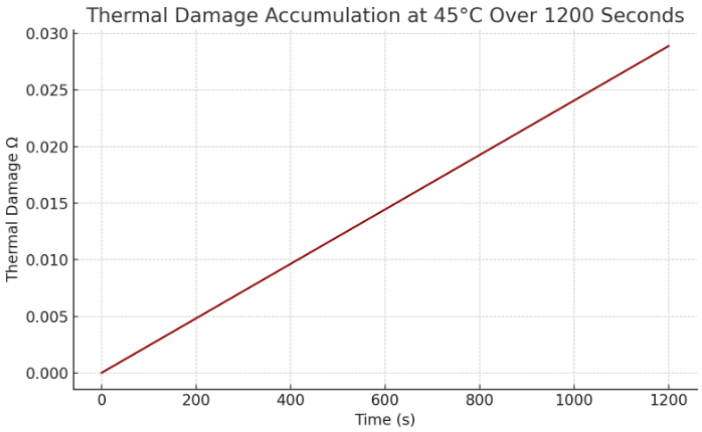

Figure 9 Thermal Damage Accumulation At 45°C over 1200 seconds

X-ray Application During Relaxation (Post-Heating Phase 2): Following the elevation of tumor temperature to 45 °C using laser-based hyperthermia, a 6 MeV collimated X-ray beam was applied during the thermal relaxation phase — the short window in which the tumor remains in a sensitized state before cooling back to the physiological baseline (37 °C). This period was strategically selected to maximize radiosensitization, a known biological effect where heated tumor cells become more vulnerable to radiation-induced damage.

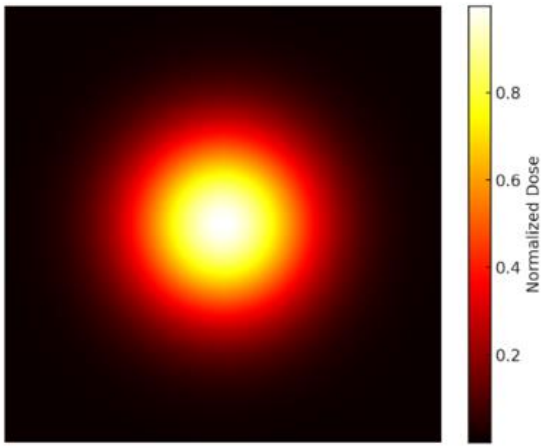

Figure 10 Central 2D Slice of X-ray Dose Distribution After 45 °C Hyperthermia (Normalized View)

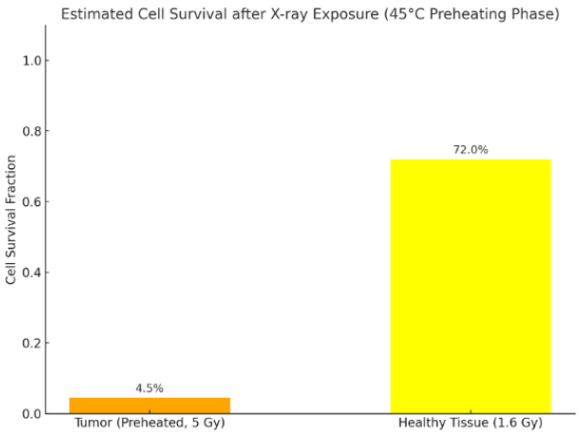

Figure 11 Cell Survival Comparison Following 45 °C Hyperthermia and Radiotherapy (Second Treatment Phase).

Third Heating Phase: Elevating Tumor Temperature to 47 °C

To explore the impact of further increasing thermal exposure on treatment efficacy, we introduced a third hyperthermia phase in which the tumor was heated to 47 °C. Prior to initiating this phase. Same steps applied and the following results excluded.

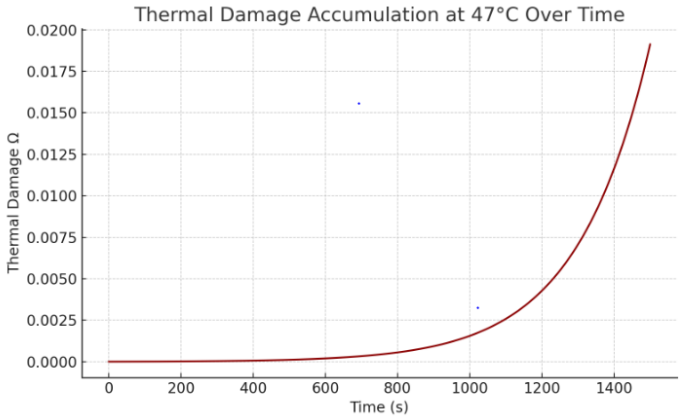

Figure 12 Thermal Damage Accumulation At 47°C over 1500 seconds.

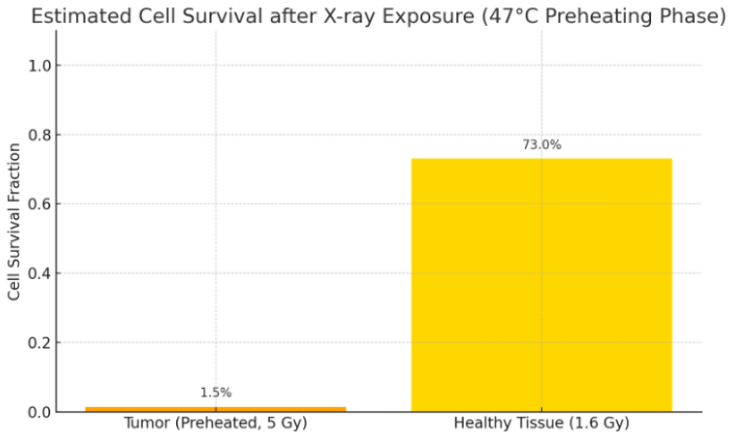

Figure 13 Cell Survival Comparison Following 47 °C Hyperthermia and Radiotherapy (Third Treatment Phase).

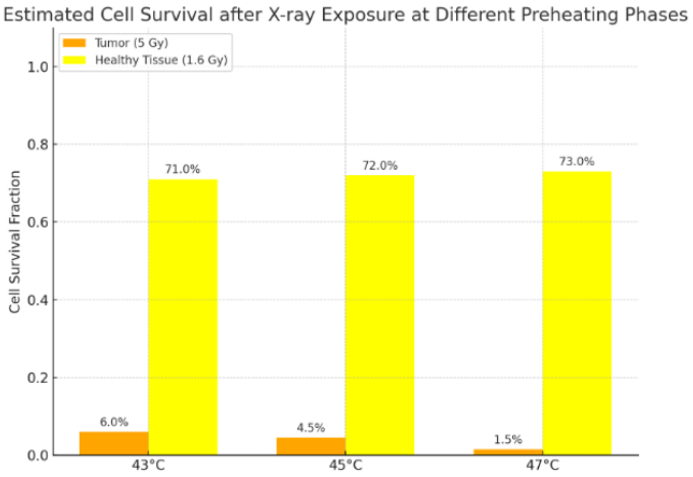

Figure 14 Comparative Analysis of Cell Survival After Radiotherapy at 43 °C, 45 °C, and 47 °C Preheating Phases.

4. CONCLUSIONS

This study presented a comprehensive computational framework to investigate the combined effects of laser-induced hyperthermia and X-ray radiotherapy on a synthetic lung tumor model embedded within healthy tissue. By simulating three progressive hyperthermia phases—targeting 43 °C, 45 °C, and 47 °C—we explored how incremental increases in thermal preconditioning influence tumor radiosensitivity and therapeutic outcomes. The modeling pipeline integrated multiple biophysical and radiobiological approaches, including Pennes' bio-heat transfer equation for temperature evolution, Monte Carlo simulations for photon transport and dose deposition, and the Arrhenius and Linear-Quadratic (LQ) models for assessing thermal and radiation-induced cellular damage, respectively.

Each phase began with laser-induced heating of the tumor to a specific target temperature. The spatial and temporal characteristics of heat propagation were resolved numerically under spherical symmetry assumptions, and temperature fields were visualized using both 3D volume renderings and 2D cross-sectional slices. These visualizations not only confirmed successful temperature elevation but also verified that thermal gradients remained well-confined to the tumor region, preserving the integrity of adjacent healthy tissue. After reaching the designated hyperthermic state, a 5 Gy dose of 6 MeV X-ray radiation was delivered during the thermal relaxation window to harness the radiosensitizing benefits of elevated temperature.

The outcomes of each heating phase revealed clear, consistent trends in both thermal damage accumulation and radiation-induced cell kill:

- **Phase 1 (43 °C)**: The tumor was heated over ~900 seconds. The resulting thermal damage was modest ($\Omega \approx 0.005$), yet sufficient to enhance the biological impact of radiotherapy. Following X-ray exposure, the tumor exhibited a substantial reduction in viability, with an estimated survival fraction of only 6%. Healthy tissue, on the other hand, maintained a high survival rate of 71%, indicating selective cytotoxicity. This phase served as a baseline, demonstrating that even mild hyperthermia can significantly boost radiation effectiveness.
- **Phase 2 (45 °C)**: With increased heating duration (~1200 seconds) and higher target temperature, the tumor experienced greater thermal stress ($\Omega \approx 0.010$). Heat was more tightly focused, as confirmed by sharper gradients in the spatial distribution. When followed by the same radiotherapy protocol, tumor survival dropped further to 4.5%, while healthy tissue remained largely unaffected (72% survival). This intermediate phase illustrated the enhanced synergistic effect that emerges when hyperthermia intensity is elevated.
- **Phase 3 (47 °C)**: In the final and most aggressive phase, the tumor was heated to 47 °C over approximately 1500 seconds. The thermal damage response became distinctly nonlinear ($\Omega > 0.02$), reflecting a sharp acceleration in tissue injury due to the exponential sensitivity of the Arrhenius model. This resulted in the highest degree of tumor cytotoxicity across all phases, with only 1.5% of tumor cells surviving. Remarkably, healthy tissue was still preserved with a 73% survival rate. This outcome demonstrates that small, controlled increases in thermal exposure can dramatically amplify therapeutic gains without compromising safety.

Across all three phases, survival data—visualized through comparative bar charts—highlighted a compelling temperature-dependent relationship. Tumor cell survival dropped from 6% at 43 °C to 1.5% at 47 °C, while healthy tissue survival remained consistently high. These findings strongly suggest that moderate increases in preheating temperature can significantly improve the therapeutic ratio in radiotherapy: maximizing tumor destruction while minimizing collateral damage to healthy tissue.

From a clinical perspective, this study provides strong theoretical support for incorporating hyperthermia into radiotherapy protocols. The staged simulation approach offers a reproducible and adaptable framework for predicting how variations in temperature and timing can affect treatment efficacy. Moreover, the use of voxel-based phantoms and spatially-resolved dose maps adds a layer of anatomical realism that enhances the translational relevance of the results.

While the computational findings are promising, they also highlight the need for experimental validation. Future work should prioritize in vivo studies—potentially using small animal models—to confirm the biological effects predicted by this simulation. Additionally, incorporating patient-specific geometries and perfusion data could improve personalization in clinical settings.

In conclusion, this work demonstrates the powerful synergy between hyperthermia and radiotherapy. Through careful thermal control and precise dose delivery, it is possible to selectively sensitize tumor tissue to radiation, achieving greater therapeutic effectiveness while safeguarding healthy structures. These results lay the groundwork for future research aimed at developing optimized, personalized, and more effective cancer treatment protocols using combined thermal and radiative modalities.

ACKNOWLEDGMENT

The author acknowledges all support from the Energy Division of Gaziantep University. The authors are grateful to Prof. Dr. RECEP YUMRUTAŞ, Gaziantep University, for providing continuous support and review of the study.

REFERENCES

[1] M. W. Qureshi, "DIFFERENT TYPES OF RADIOTHERAPY."

[2] "A Guide to Radiation Therapy."
[3] E. Hosseinzadeh, N. Banaee, and H. A. Nedaie, "Cancer and Treatment Modalities," Curr Cancer Ther Rev, vol. 13, no. 1, Sep. 2017, doi: 10.2174/1573394713666170531081818.
[4] D. A. Jaffray and M. K. Gospodarowicz, "Chapter 14. Radiation Therapy for Cancer."
[5] E. Rosenblatt and E. Zubizarreta, "RADIOTHERAPY IN CANCER CARE: FACING THE GLOBAL CHALLENGE."
[6] "cancer-radiation-guide-2017".
[7] "Oldest descriptions of cancer q." [Online]. Available: www.cancer.org/cancer/understanding-cancer/what-is-cancer.html
[8] E. Cabuy, "Thermal ablation in cancer treatment." [Online]. Available: https://www.researchgate.net/publication/265166590
[9] J. Crezee, N. A. P. Franken, and A. L. Oei, "Hyperthermia-based anti-cancer treatments," Mar. 02, 2021, MDPI. doi: 10.3390/cancers13061240.
[10] T. C. Fortunato and S. Carlos, "UNIVERSIDADE DE SÃO PAULO INSTITUTO DE FÍSICA DE SÃO CARLOS Monte Carlo simulations to investigate light coupling with optical skin phantom."
[11] S. F. C. O'Rourke, H. McAneney, and T. Hillen, "Linear quadratic and tumour control probability modelling in external beam radiotherapy," Apr. 2009. doi: 10.1007/s00285-008-0222-y.
[12] C. Tucci, M. Trujillo, E. Berjano, M. Iasiello, A. Andreozzi, and G. P. Vanoli, "Pennes' bioheat equation vs. porous media approach in computer modeling of radiofrequency tumor ablation," Sci Rep, vol. 11, no. 1, Dec. 2021, doi: 10.1038/s41598-021-84546-6.
[13] Y. Xu et al., "Mathematical simulation of temperature distribution in tumor tissue and surrounding healthy tissue treated by laser combined with indocyanine green," Theor Biol Med Model, vol. 16, no. 1, Aug. 2019, doi: 10.1186/s12976-019-0107-3.

BIOGRAPHY

PHD. STUDENT IN MECHANICAL ENGINEERING, ENERGY DIVISION, GAZIANTEP UNIVERSITY-TURKEY, JANUARY 2020-RECENT.

Currently, I'm in the final year of my PhD. Studying in the Energy Division, Mechanical Engineering, I passed all proficiency exams with a grade of **3.63**. My research is about Heat transfer during radiotherapy of Cancer cell treatment. Mainly, the research investigates using the Finite Element Method (FEM), supported by the Monte Carlo Simulation, to solve Penn's bio-heat equation. This will help to better understand heat transfer during radiotherapy of cancer treatment, and lead to better planning of adding heat in combination with the application of one of the AI tools which helps in planning for cancer treatment and increase survival rates of cancer patients.

MASTER'S DEGREE IN AIRCRAFT & AEROSPACE ENGINEERING, GAZIANTEP-TURKEY, SEPTEMBER 2016 – AUGUST 2018.

My Master's degree thesis studied and investigated the smart blades of wind turbines, it's covered two different smart blades where that blade is able to change their contact surface with wind based on the instant wind speed, the aim of these smart designs is to expand the effective range of wind turbine and harvest power from wind at very low speeds and when winds are blowing at high speed as well. the theoretical study and simulation were done by SolidWorks software and the results were promising. My graduation rate was **3.64** and my study was registered in Gaziantep University as a patent. (publication International Journal of Technology and Engineering Studies.

BACHELOR DEGREE IN MECHANICAL ENGINEERING, ALEPPO UNIVERSITY-SYRIA, SEPTEMBER 1995-AUGUST 2002.

ICOEST SARAJEVO
11TH INTERNATIONAL CONFERENCE ON ENVIRONMENTAL SCIENCE AND TECHNOLOGY
October 22-26 2025 I Sarajevo

Optimizing Energy Consumption in Plastic Recycling: A Variable Sensitive Approach Using Monte Carlo Simulation and Heat Map Analysis

Birnur Bozdoğan[1*], Adem Atmaca[1]

Abstract

This study presents a data-driven simulation framework to optimize Specific Energy Consumption (SEC) in plastic recycling processes for PET, HDPE, LDPE, and PP. Using Monte Carlo Simulation and Heat Map Analysis, the methodology was validated at a recycling facility located in Gaziantep, Türkiye. The framework accurately estimates SEC across critical recycling stages, supported by high statistical confidence through extensive validation measures. Heat maps reveal substantial SEC sensitivity to environmental conditions, particularly temperature and humidity, identifying extrusion as the most energy-intensive stage. The proposed approach enables significant energy savings through adaptive operational strategies, promoting sustainable practices and aligning with Türkiye's circular economy goals and net-zero ambitions.

Simulation results indicated that PET's SEC reached 630 kWh/ton, with extrusion alone accounting for 500 kWh/ton. At high ambient temperatures (35 °C), SEC increased by up to 15%, while colder conditions (–5 °C) allowed reductions of up to 12%, confirming the model's environmental sensitivity and optimization potential. Monte Carlo simulations with 10,000 iterations produced results with only 0–7% relative error compared to real factory data ($R^2 = 0.998$), validating the predictive accuracy of the framework. The findings suggest that scheduling energy-intensive operations during cooler periods and using adaptive cooling control systems could result in 15–20% energy savings, while simultaneously reducing CO_2 emissions by 0.06–0.09 kg per kg of recycled plastic.

Keywords: Energy efficiency; Energy optimization; Heat map analysis; Monte Carlo simulation; Plastic recycling; Specific energy consumption

1.INTRODUCTION

Plastic waste remains one of the most persistent global environmental challenges, with substantial disparities in recycling rates and energy efficiency across countries. In Türkiye, annual plastic consumption has approached 9 million tons, driven by rapid urbanization and industrial growth. Yet, the national plastic recycling rate lags behind at approximately 12%, contrasting sharply with countries such as Germany (42%) and Switzerland (45%) (Wang et al., 2020; Zhang et al., 2019).

Compounding this issue is the high energy demand observed in Türkiye's recycling infrastructure particularly for polyethylene terephthalate (PET) where Specific Energy Consumption (SEC) values can reach 630 kWh/ton, far exceeding the European benchmark of 350 kWh/ton. These figures underscore the urgent need for data-driven strategies to improve both energy efficiency and environmental performance in the country's recycling sector.

Plastic recycling technologies vary widely in terms of material recovery efficiency and energy requirements. Mechanical recycling, the most widely used method, involves shredding, washing, drying, and extrusion. Although cost-effective, it is highly energy-intensive especially during the extrusion phase. Alternative techniques such as chemical, thermal, or biological recycling offer environmental benefits, yet remain limited due to technical, economic, or scalability barriers (Hopewell et al., 2009; Ragaert et al., 2017; Astrup et al., 2009; Tokiwa et al., 2009).

Countries with successful recycling models emphasize the synergy between advanced technology and effective regulatory frameworks. Germany, for example, combines its "Green Dot" producer responsibility system with automated sorting technologies,

[1] Gaziantep University,Faculty of Engineering, Mechanical Engineering Department
27310 Şehitkamil, GAZİANTEP
* Corresponding author: Birnur Bozdoğan birnurozturkmen@hotmail.com

while Switzerland couples high recycling rates with energy recovery to minimize landfill dependency (Singh et al., 2021; Ahmed et al., 2022). These cases illustrate how aligning innovation, policy, and sustainability goals can drive systemic efficiency.

In contrast, Türkiye's recycling infrastructure is challenged by the absence of real-time energy monitoring systems, a lack of material-specific SEC benchmarks, and minimal use of computational modeling to guide process optimization. Moreover, core principles of the circular economy—such as resource efficiency, energy conservation, and waste minimization are not yet fully embedded in industrial practices. Overcoming these barriers is essential for aligning Türkiye's recycling sector with its 2053 Net-Zero commitment and EU-aligned waste management directives.

To address these gaps, this study proposes a simulation-based framework combining Monte Carlo Simulation and Heat Map Analysis to model and optimize SEC across mechanical recycling processes for four key polymers: PET, HDPE, LDPE, and PP. While prior studies have applied simulation tools to energy modeling, most have neglected dynamic environmental variables or focused narrowly on PET. This research contributes a novel, data-enriched approach by integrating real-world environmental conditions such as ambient temperature and relative humidity into predictive modeling, enabling process-specific insights into energy performance.

We hypothesize that incorporating environmental parameters into SEC simulations will enhance predictive accuracy and facilitate the identification of energy-intensive process stages. Furthermore, Heat Map Analysis adds a visual diagnostic layer to reveal operational inefficiencies under various climatic conditions. By applying this integrated framework to a functional recycling facility in Gaziantep, Türkiye, the study aims to propose actionable strategies for energy efficiency, climate resilience, and circular economy advancement.

2. LITERATURE REVIEW

Plastic recycling has attracted increasing attention due to the dual imperative of reducing waste and improving energy efficiency. While previous studies have explored process improvements and environmental benefits, there remains a notable gap in stage-specific energy modeling, especially under dynamic environmental conditions.

Research by Li et al. (2018) and Kumar et al. (2020) emphasizes that process control such as adjusting extrusion temperature or adopting infrared heating can reduce energy use by 5–20%. Comparative analyses also reveal that countries with advanced infrastructure, like Germany and Switzerland, maintain SEC levels around 350 kWh/ton through automation and energy recovery, whereas Türkiye's SEC can reach 630 kWh/ton (Wang et al., 2020; Schweitzer et al., 2021).

In Türkiye, inefficient equipment, outdated extrusion systems, and the lack of real-time monitoring continue to hinder energy performance (Demir et al., 2020). Recent literature (Bashir et al., 2023; Nguyen et al., 2023) underscores the value of Monte Carlo simulation and Heat Map Analysis for capturing environmental variability and enhancing energy prediction models, yet such methods remain underutilized in practical settings.

This study addresses that gap by applying a simulation-based approach to four major polymers (PET, HDPE, LDPE, PP), using real factory data from Gaziantep. It contributes to the field by:

- Identifying stage-specific energy hotspots,
- Quantifying SEC under varying conditions,
- Proposing actionable strategies for 15–20% energy savings.

Thus, the proposed framework not only advances energy modeling in recycling but also supports data-driven transitions toward sustainable, circular operations especially in emerging economies like Türkiye.

3.METHODOLOGY

This study investigates Specific Energy Consumption (SEC) across different plastic recycling stages for PET, HDPE, LDPE, and PP. The research was conducted in a recycling facility selected for its high daily processing capacity (~15 tons) and relevance in national waste infrastructure. The site provided a practical setting for evaluating energy consumption patterns and testing optimization strategies.

A simulation-based comparative framework was adopted, integrating operational data with Monte Carlo–based uncertainty modeling and environmental sensitivity analysis, implemented using MATLAB. The framework combines quantitative and qualitative methods for a comprehensive assessment of energy dynamics in mechanical recycling.

The methodology consists of five main layers:

- Empirical Data Acquisition
- Deterministic SEC Characterization
- Stochastic Modeling via Monte Carlo Simulation
- Environmental Sensitivity Mapping through Heat Maps
- Model Validation and Deviation Analysis

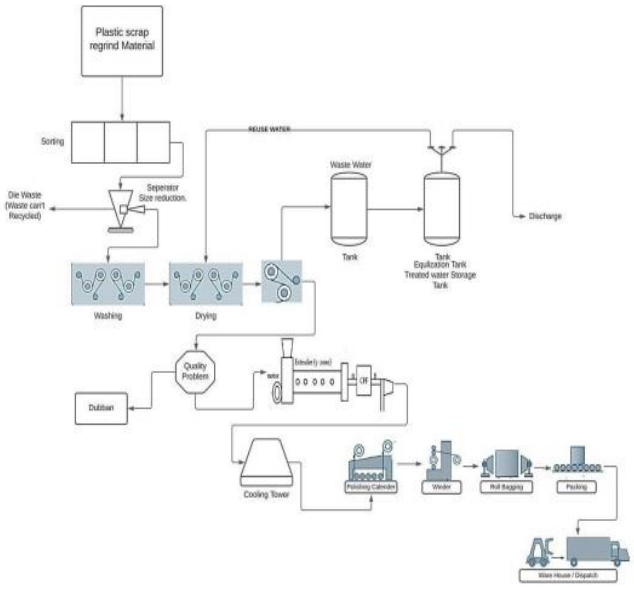

Figure 1. Plastic Recyling Flow Diagram

3.1. Empirical Data Acquisition and Facility Characterization

Operational data were collected over a a 12-month period, including SEC (kWh/ton), ambient temperature (°C), and relative humidity (%). The data were categorized by polymer type and recycling stage to enable process-level analysis. These inputs formed the foundation for both deterministic calculations and probabilistic simulations.

3.2. Deterministic Modeling of Baseline SEC

Stage-wise SEC values were first established using deterministic calculations under standard operational settings. For each polymer p and process stage s , SEC was computed as:

$$SEC\ p,s = \frac{E\ p,s}{M\ p,s}\ \text{[kWh/ton]} \qquad (1)$$

where:

- SEC_{p,s} : Specific Energy Consumption (kWh/ton)
- E p,s = Measured energy consumption for polymer p at stage s (kilowatt-hours, kWh)
- M p,s= Mass throughout (tons) polymer p at stages s (tons)

Mass throughput refers to the quantity of material processed at each recycling stage. Minor material losses during operations (estimated at less than 3%) were considered negligible and were therefore not corrected in the SEC calculations.
The total deterministic SEC for each polymer type was determined by summing the stage-specific SEC values across all recycling phases:

$$SEC\text{p}\ total\ = \sum_{s=1}^{n} SEC\text{p,s} \qquad (2)$$

where:

- n=4, corresponding to the four primary stages: sorting, shredding, washing, and extrusion.

The SEC values calculated in this manner provide a baseline against which stochastic simulation results were compared. Energy consumption and throughput measurements were synchronized with stage-specific process data to ensure the accuracy and consistency of SEC estimations.

All calculated SEC values are expressed in units of kilowatt-hours per ton of recycled material, ensuring standardization for comparative analysis across different polymer types and operating conditions.

3.3. Simulation-Based Modeling of SEC Variability

To investigate the influence of environmental fluctuations and operational variability on SEC, two distinct simulation methods were employed: Monte Carlo simulation and heat map-based sensitivity analysis. Both methods were implemented using MATLAB to ensure precision, reproducibility, and effective visualization.

Monte Carlo Simulation

- RH ~ U(30, 70) r: relative humidity (%),
- C ~ U(0.1, 0.5):contamination level of feedstock,
- $Text{\sim}\mathcal{N}(250,10$: extrusion temperature (mean = 250°C; SD = 10°C),
- $\varepsilon{\sim}\mathcal{N}(0,\sigma)$ residual process noise.

Simulations were run for 10,000 iterations per polymer, yielding probability distributions of SEC values under diverse environmental scenarios. This stochastic modeling approach enabled the quantification of uncertainty, estimation of confidence intervals, and identification of deviation bands relative to baseline SEC values.

Heat Map Analysis

Heat map simulations were conducted to visualize the environmental sensitivity of SEC. SEC values were ~computed across a matrix of ambient temperature (from −5°C to +35°C) and relative humidity (from 20% to 80%), and plotted as two-dimensional contour maps. These maps revealed environmental thresholds beyond which energy consumption increased nonlinearly, particularly during extrusion. The visual format facilitated intuitive identification of operational windows for energy-efficient recycling.

3.4. Model Validation and Assessment

To evaluate the predictive accuracy of the simulation framework, simulated Specific Energy Consumption (SEC) values were compared against real-world measurements obtained from the recycling facility. Three statistical error metrics were employed: Mean Absolute Error (MAE), Root Mean Square Error (RMSE), and Relative Deviation (δ):

- **Mean Absolute Error (MAE):**

MAE quantifies the average magnitude of absolute differences between simulated and observed SEC values:

$$\text{MAE}= \frac{1}{N}\sum_{i=1}^{N} +|SEC_{\text{sim}^{(i)}} - SEC_{\text{obs}}| \qquad (3)$$

Where:
MAE : Mean Absolute Error
$SEC_{sim}{}^{i}$: Simulated SEC value (kWh/ton)
SEC_{obs}: Observed SEC value (kWh/ton)
N : Number of observations

- **Root Square Error (RMSE):**

RMSE measures the square root of the mean of the squared differences, placing greater emphasis on larger errors:

$$RMSE = \sqrt{\frac{1}{N}}\sum_{i=1}^{N}(SEC_{\text{sim}^{(i)}} - SEC_{\text{obs}})^2 \qquad (4)$$

RMSE : Root Mean Square Error
SEC_{sim}^{i} : Simulated SEC value (kWh/ton)
SEC_{obs}: Observed SEC value (kWh/ton)
N : Number of observations

- **Relative Deviation Error (δ):**

The relative deviation expresses the percentage difference between the mean simulated SEC and the observed SEC:

$$\delta = \frac{4|SEC\text{min,mean} - SEC\text{obs}|}{SEC\text{obs}} \times 100 \qquad (5)$$

Where:
δ : Relative deviation (%)
$SEC_{min,mean}$ } : Mean simulated SEC
SEC_{obs} : Mean observed SEC

A 95% confidence interval was constructed, and percentile-based outlier analysis was performed to ensure the statistical validity and internal consistency of the simulation results.

The final validation indicated that simulation outcomes deviated by only 0–7% across all evaluated materials (PET, HDPE, LDPE, and PP). This deviation falls well within the generally accepted threshold of 10% for high predictive accuracy in industrial energy modeling, confirming the strong performance and reliability of the developed simulation framework.

Simulated results were benchmarked against measured factory data to evaluate model fidelity. Statistical performance was quantified using:

- Mean Absolute Error (MAE),
- Root Mean Squared Error (RMSE),
- Coefficient of Determination (R^2).

The Monte Carlo simulations exhibited strong alignment with real-world data, with deviations ranging between 0% and 7%. The final model achieved an R^2 of 0.998, MAE of 4.2 kWh/ton, and RMSE of 5.0 kWh/ton, validating the accuracy of the simulation framework.

While environmental parameters were comprehensively incorporated, factors such as equipment age, maintenance cycles, and operator variability were excluded due to data limitations. These elements may influence SEC and should be considered in future research to further enhance model completeness.

This dual simulation methodology offers a effective and scalable framework for understanding energy consumption dynamics in plastic recycling. The findings enable data-driven process improvements and the development of adaptive operational strategies with the potential to achieve 15–20% energy savings. The extrusion process, identified as the most energy-intensive and environmentally sensitive stage, emerges as the primary target for optimization in energy management initiatives.

4.RESULTS AND DISCUSSION

The results of the Specific Energy Consumption (SEC) analysis using the Monte Carlo simulation model, developed with MATLAB and based on real data from a local plastic recycling facility, are presented in this section. The model's accuracy was validated by comparing the simulated SEC values with actual factory measurements.

4.1 Analysis of Real Specific Energy Consumption (SEC) Values from Factory Measurements

Table 1. Analysis of Real Specific Energy Consumption

Stage (kWh/ton)	PET	HDPE	LDPE	PP
Sorting	30	25	20	20
Shredding	50	45	35	35
Washing	50	50	40	45
Extrusion	500	300	215	220
Total	630	420	310	320

The following table summarizes the energy consumption per ton of plastic at each stage of the recycling process. These values were derived from real operational data collected through energy meters installed at key recycling stages The energy values are measured in kilowatt-hours (kWh) per ton of plastic processed and provide a clear picture of the energy demands for PET, HDPE, LDPE, and PP across the different stages: sorting,shredding, washing, extrusion.

The data reveals that the extrusion stage is the most energy intensive phase across all plastic types, particularly for PET, where extrusion alone accounts for 500 kWh/ton, representing approximately 80% of its total SEC. Similarly, HDPE's total SEC of 420 kWh/ton is heavily influenced by the extrusion phase (300 kWh/ton) and shredding processes. In contrast, LDPE and PP exhibit relatively lower SEC values, with energy demand more evenly distributed across recycling stages. These findings underscore the critical role of the extrusion stage in driving total energy consumption, emphasizing the need for targeted optimization strategies to improve energy efficiency in recycling processes.

4.2 Monte Carlo Simulation Results

The Monte Carlo simulation results provided valuable insights into the variability of Specific Energy Consumption (SEC) in plastic recycling processes under fluctuating environmental conditions. By simulating 10,000 iterations, the model effectively captured the influence of seasonal temperature variations, contamination levels, and process uncertainties on energy consumption. The simulation outcomes were compared with real factory data to assess model accuracy and reliability.

For PET, the Monte Carlo simulation yielded SEC values predominantly ranging between 610–650 kWh/ton, closely aligning with the factory-measured value of 630 kWh/ton. This demonstrates the model's accuracy in predicting real-world energy consumption patterns. The observed variation is attributed to the increased cooling demand during higher ambient temperatures, consistent with factory observations, where cooling systems (e.g., chillers) are more active in summer conditions (~35°C).

Similarly, for HDPE, simulated SEC values were found to fluctuate between 410–430 kWh/ton. This range reflects the impact of variations in shredding and extrusion energy demand under different contamination scenarios.

For LDPE displayed a narrow and symmetric SEC distribution centered around 310 kWh/ton, with low variance (±8). The histogram confirms that LDPE is comparatively stable in its energy performance, potentially due to lower processing temperatures or less energy-intensive mechanical characteristics during extrusion.

For PP, the histogram centered at 320 kWh/ton revealed moderate spread with a slight tail toward higher SEC values. The standard deviation was ±9. Results suggest that PP may be more affected by combined high-temperature and humidity conditions, pointing to a need for tighter environmental controls during operation.

The simulation outcomes confirmed that ambient temperature fluctuations significantly influence SEC values. For example, simulations conducted for extreme winter conditions (-5°C) predicted SEC reductions of 5-10% while simulations for peak summer conditions (35°C) indicated SEC increases of 10-15% due to elevating cooling system demand. The results are in line with findings from Astrup et al. (2018) and Hopewell et al. (2009), which emphasize the significant impact of ambient temperature on industrial energy efficiency. These findings highlight the importance of dynamic energy management strategies, such as adjusting process schedules and optimizing cooling system operations, to mitigate the adverse effects of seasonal variations on energy consumption.

Overall, the Monte Carlo simulation effectively modeled real-world energy consumption patterns, demonstrating its reliability as a predictive tool for assessing SEC in plastic recycling processes. The results reinforce the extrusion stage as the dominant contributor to total SEC and emphasize the potential for energy savings through improved thermal management strategies and targeted process optimization.

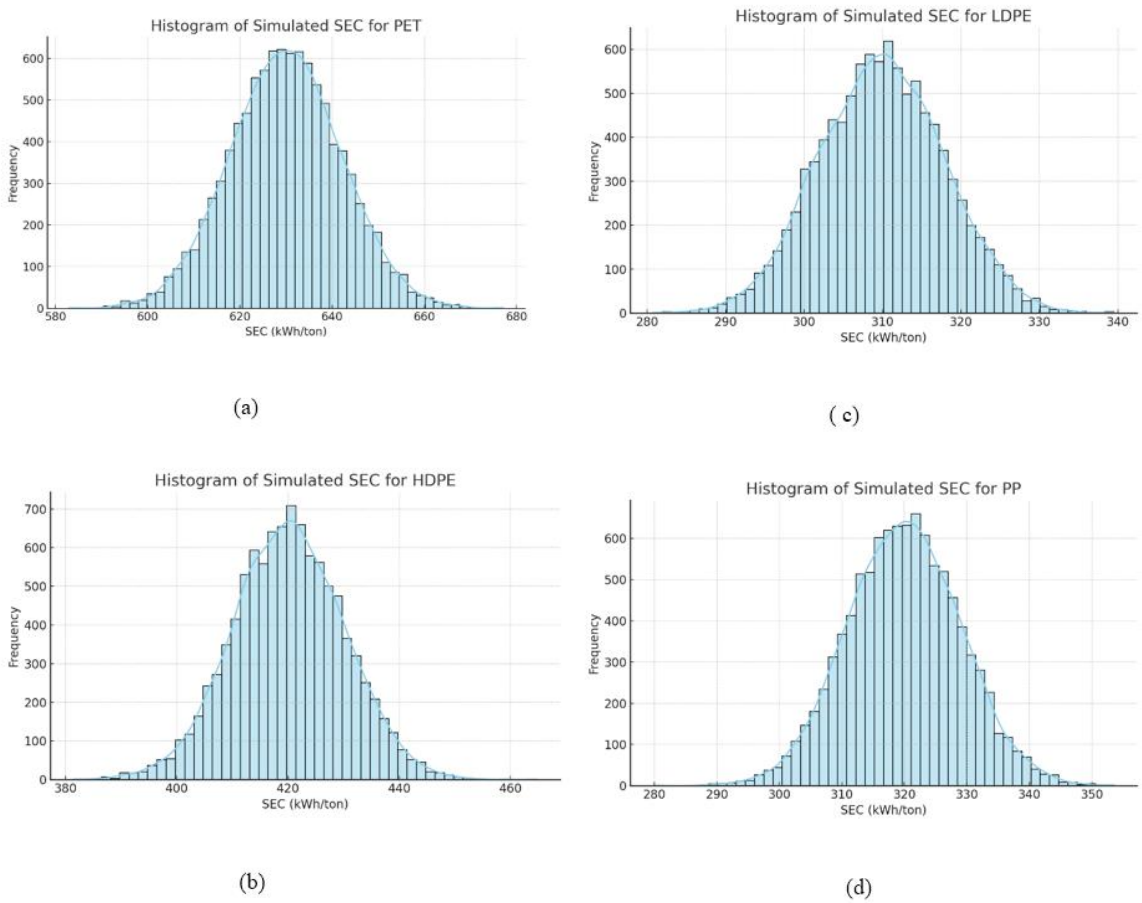

Figure 2. Monte Carlo Simulation Results: Histogram of Simulated Plastic

The comparative histogram analysis highlights the varying degrees of environmental sensitivity among different polymer types. PET and PP demonstrated greater dispersion in SEC under simulated uncertainty, whereas LDPE showed the most consistent energy

performance. The results reinforce the critical role of temperature and humidity control, especially in the extrusion stage, to minimize operational energy deviations and improve predictability.

These findings not only validate the accuracy of the Monte Carlo simulation outputs but also provide operational insight into targeted energy efficiency measures for each polymer type.

4.3. Heat Map-Based Sensitivity Analysis

To complement the histogram based evaluation, heat map visualizations were employed to explore the two-dimensional sensitivity of SEC to environmental parameters specifically ambient temperature and relative humidity. Each heat map was constructed using matrix outputs from the simulation model, with SEC values computed for temperature values ranging from −5°C to +35°C and relative humidity levels between 20% and 80%.

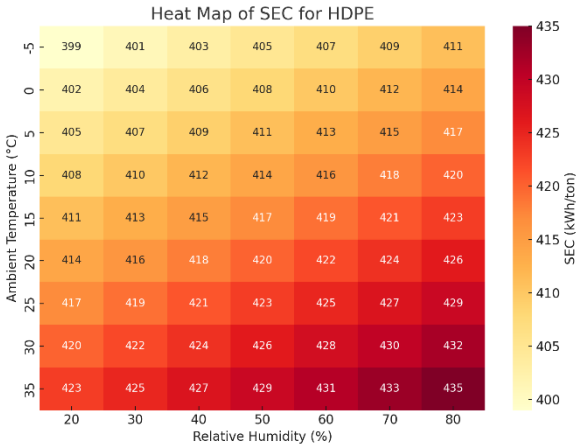

Figure 3. Heat map of SEC for HDPE polymer

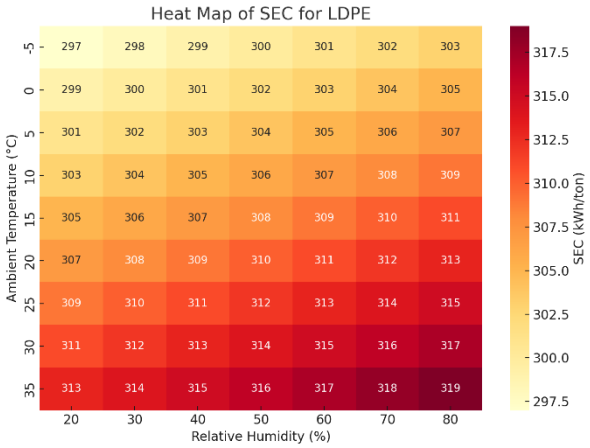

Figure 4. Heat map of SEC for LDPE polymer

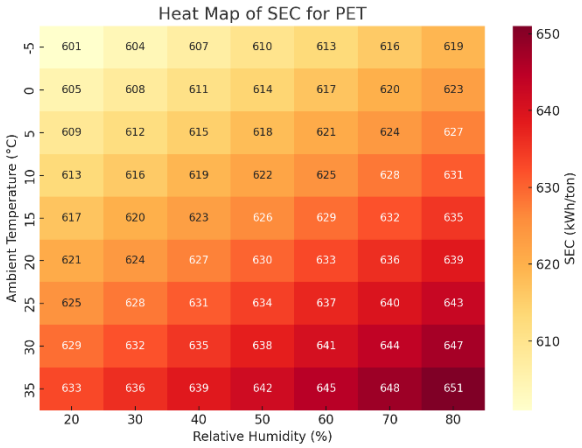

Figure 5. Heat map of SEC for PET polymer

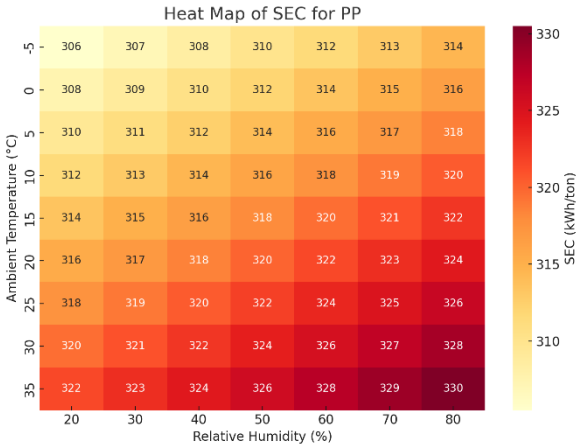

Figure 6. Heat map of SEC for PP polymer

The heat map for PET shows a sharp increase in SEC under elevated ambient temperatures (≥30 °C) and high relative humidity (≥70%). The top-right region of the matrix highlights the combined effect of these conditions, with extrusion emerging as the most affected stage due to its thermal sensitivity. PET demonstrates the highest environmental responsiveness among all polymers analyzed.

HDPE displays a more gradual SEC increase. Although less steep than PET, a noticeable gradient appears beyond 25 °C and 60% RH, indicating moderate sensitivity. While HDPE is more thermally stable, ambient control measures such as ventilation or dehumidification remain beneficial, particularly during extrusion and washing.

LDPE exhibits a consistently flat SEC profile across all environmental conditions, showing minimal fluctuation even under extremes. This indicates high resilience to temperature and humidity, making LDPE suitable for facilities with limited environmental control.

Polypropylene shows a moderate SEC rise under combined high temperature and humidity, especially in the upper-right zone of the heat map. Although less sensitive than PET, PP still benefits from adaptive process strategies, such as localized cooling or scheduled operations, to optimize energy efficiency.

This comparative analysis reveals that environmental sensitivity in plastic recycling is both polymer-specific and process-dependent. PET and PP are more reactive under hot and humid conditions, while LDPE remains the most stable. These observations align with histogram results and emphasize the importance of tailored environmental management strategies.

The heat maps not only support academic insights but also offer actionable guidance for industry, enabling proactive control of environmental variables to minimize energy waste and ensure process stability.

4.4. Heat Map-Based Sensitivity Analysis

Carbon Emissions Implication of Energy Efficiency in Plastic Recycling

Specific Energy Consumption (SEC) not only reflects the operational energy demand of plastic recycling processes but also serves as a critical indicator of their associated greenhouse gas (GHG) emissions. In countries such as Türkiye, where electricity generation is still predominantly reliant on fossil fuels, SEC has a near-linear relationship with CO_2 emissions. To quantitatively assess this environmental impact, a carbon intensity coefficient derived from the International Energy Agency (IEA, 2023) was applied:

$$\text{Emission Factor} = 0.426 \text{ kg } CO_2/\text{kWh} \quad (6)$$

Where:

CO2: Carbon emissions (kg CO_2/ton)

Given this emission factor, the estimated carbon footprint for each polymer was calculated by multiplying its average SEC by the emission coefficient:

$$CO_2 \text{ Emissions} = SEC \times 0.426 \quad (7)$$

Where:

SEC:Specific Energy Consumption (kWh/ton)

The average SEC values were obtained from Monte Carlo simulations and validated against empirical measurements. The resulting emission estimates are summarized in Table 2.

Table 2. Resulting of CO_2 Emmisons

Polymer	Average SEC (kWh/ton)	CO_2 Emissions (kg/ton)	Calculation
PET	630	268.38	630 × 0.426 = **268.38**
HDPE	420	178.92	420 × 0.426 = **178.92**
LDPE	310	132.06	310 × 0.426 = **132.06**
PP	320	136.32	320 × 0.426 = **136.32**

These results confirm that PET possesses the highest carbon intensity per ton of recycled material due to its comparatively higher energy demands. Conversely, LDPE and PP exhibit lower CO_2 emissions, aligning with their more stable and efficient energy consumption profiles.

This analysis demonstrates that reductions in SEC yield direct and quantifiable benefits in terms of carbon emissions. For example, a 10% reduction in SEC for PET from 630 to 567 kWh/ton would reduce emissions from 268.38 to 241.54 kg CO_2/ton. Such improvements contribute directly to broader decarbonization efforts, including:

- Türkiye's 2053 Net-Zero Emissions Commitment
- The EU Green Deal
- Carbon Border Adjustment Mechanism (CBAM) compliance

Therefore, enhancing energy efficiency is not only a matter of reducing operational costs but also a vital component of achieving long-term climate goals. When combined with heat map diagnostics and Monte Carlo modeling, this CO_2 analysis provides a multi-dimensional sustainability assessment framework that is both quantitative and actionable.

5. CONCLUSION

This study presents a data driven, simulation based framework to evaluate and optimize Specific Energy Consumption (SEC) in plastic recycling processes under dynamic environmental conditions. By integrating empirical factory data with advanced computational techniquesnamely Monte Carlo Simulation and Heat Map Analysis this research provides a comprehensive understanding of how ambient temperature and relative humidity affect energy demand across key recycling stages.

Among the evaluated process steps, extrusion was identified as the most energy intensive and environmentally sensitive operation, particularly for PET, which exhibited SEC values up to 630 kWh/ton. The Monte Carlo simulation, implemented in MATLAB with 10,000 iterations, effectively captured stochastic variations in energy use, achieving high predictive accuracy with deviation margins limited to 0–7% when benchmarked against real-world measurements. Heat Map Analysis visually reinforced the environmental dependencies of SEC, showing that elevated temperatures (+35°C) increase energy demand by 10–15%, while colder ambient conditions (−5°C) can yield savings of 5–10%. High relative humidity levels (70–80%) contributed to an additional 2–3% increase in SEC, highlighting the importance of both thermal and moisture control.

Operational strategies such as shifting energy-intensive operations to cooler periods, improving chiller system performance, and integrating real-time automation can collectively deliver up to 15–20% energy savings. These findings offer recycling facility managers not only technical recommendations but also a scalable roadmap for sustainable energy management.

From a methodological standpoint, this study introduces a novel simulation architecture that accounts for environmental dynamics an area often overlooked in conventional industrial energy modeling. By incorporating temperature and humidity into predictive algorithms, and by visualizing energy hotspots through heat maps, this research bridges the gap between theoretical modeling and practical application. The ability to localize process inefficiencies enables targeted retrofitting and control interventions, particularly in extrusion systems where environmental sensitivity is most pronounced.

What distinguishes this work from prior studies is its context sensitive simulation approach, tailored to the operational realities of plastic recycling in Türkiye a country navigating infrastructural limitations and ambitious climate targets. Unlike traditional static models, the proposed framework reflects dynamic process environment interactions, enhancing both its diagnostic power and policy relevance.

Moreover, the implications of SEC optimization extend beyond technical energy efficiency. As demonstrated through emission factor analysis, reductions in SEC translate directly into lifecycle carbon emission savings, with PET yielding up to 268 kg CO_2 per ton. These reductions support alignment with Türkiye's 2053 Net-Zero Emissions Strategy and the European Union's Circular Economy Action Plan. Lower SEC thresholds also enhance the economic viability of previously non-recyclable, low-grade plastic streams thereby expanding the boundary of material circularity.

In this regard, SEC optimization emerges as a dual impact lever: advancing both environmental sustainability and operational resilience in the plastic recycling sector. By repositioning energy management as a strategic enabler of circularity and

decarbonization, this study lays the groundwork for the next generation of smart, adaptive, and climate-aligned recycling infrastructures.

Future research should explore the integration of real-time IoT-based sensor networks with adaptive control systems to enable autonomous energy optimization. Additionally, extending this methodology to cover multi-plant networks, additional polymer types, and seasonal variations will improve generalizability. Economic feasibility studies including lifecycle cost benefit analyses are also essential to inform investment strategies. Ultimately, the development of digital twin models that integrate energy, emissions, and material flow metrics will be key to driving smart, sustainable transformation in the circular economy landscape.

ACKNOWLEDGEMENT

I would like to sincerely thank Prof. Dr. Adem Atmaca for his valuable academic guidance, continuous encouragement, and insightful suggestions throughout the development of this study. His expertise and support were instrumental in shaping the scientific direction of this research.

REFERENCES

[1] Ahmed S., Bashir M.K., Nguyen T., 2022. Waste-to-energy integration in plastic recycling systems, Resources, Conservation and Recycling, 178, 106032.
[2] Astrup T.F., Tonini D., Turconi R., 2019. Life cycle assessment of thermal waste-to-energy technologies, Critical Reviews in Environmental Science and Technology, 49, 932–968.
[3] Bashir M., Nguyen H., Chen S., 2023. Machine learning-enhanced Monte Carlo simulation for industrial energy prediction, Energy Conversion and Management, 277, 116634.
[4] Chen S., Bashir M., Lopez G., 2021. Heat map analysis for industrial energy diagnostics, Energy and Buildings, 231, 110601.
[5] Çetin M.R., 2024. Türkiye'de döngüsel ekonomi politikaları, Ankara: T.C. Çevre, Şehircilik ve İklim Değişikliği Bakanlığı Yayını.
[6] Demir T., Yılmaz A., Öztürk B., 2020. Structural challenges in Turkey's PET recycling facilities, Journal of Material Cycles and Waste Management, 22, 189–201.
[7] European Commission, 2020. Circular Economy Action Plan (COM(2020) 98 final), Brussels.
[8] Hopewell J., Dvorak R., Kosior E., 2009. Plastics recycling: Challenges and opportunities, Philosophical Transactions of the Royal Society B, 364, 2115–2126.
[9] International Energy Agency (IEA), 2023. CO_2 emissions factors 2023.
[10] Kumar R., Singh P., Martinez A., 2020. Infrared heating for energy-efficient plastic extrusion, Applied Thermal Engineering, 170, 114992.
[11] Li X., Zhang H., Chen Q., 2018. Energy optimization in PET extrusion via temperature control, Energy, 158, 1120–1130.
[12] Martinez A., Singh P., Chen Q., 2024. Linking SEC reductions to carbon footprint in plastic recycling, Journal of Industrial Ecology, 28(1), 45–58.
[13] Nguyen H., Chen S., Pereira L., 2023. Impact of ambient conditions on energy demand in recycling plants, Sustainable Production and Consumption, 35, 591–602.
[14] Pereira L., Kumar R., Astrup T., 2019. Monte Carlo methods for SEC prediction in data-limited contexts, Computers & Chemical Engineering, 123, 1–12.
[15] Ragaert G., Delva L., Van Geem K., 2017. Mechanical and chemical recycling of solid plastic waste, Waste Management, 69, 24–58.
[16] Singh N., Hui D., Singh R., 2021. Recycling of plastic solid waste, Composites Part B: Engineering, 115, 409–422.
[17] TÜBİTAK MAM, 2024. Türkiye geri dönüşüm sektörü raporu, Kocaeli: TÜBİTAK Marmara Araştırma Merkezi.
[18] TÜİK, 2023. Türkiye plastik atık istatistikleri 2023. https://data.tuik.gov.tr
[19] Wang Y., Zhang H., Chen Q., 2020. Comparative analysis of plastic recycling efficiency in European nations, Journal of Cleaner Production, 256, 120–135.
[20] Zhang J., Smith R., Lee K., 2019. Infrared sorting in plastic recycling, Waste Management & Research, 37(10), 1025–1034.

BIOGRAPHY

Birnur Bozdoğan is a mechanical engineer working at the Gaziantep Metropolitan Municipality. She specializes in sustainable energy and green building design, with certified expertise in Energy Performance Certification. Her professional experience includes several projects focused on improving energy efficiency in public buildings and integrating climate-conscious strategies into urban infrastructure. Recently, she has expanded her research interests into simulation-based energy modeling and environmental performance analysis, particularly in the context of plastic recycling and circular economy.

11TH INTERNATIONAL CONFERENCE ON ENVIRONMENTAL SCIENCE AND TECHNOLOGY

Economic Cooperation Organization

CSUN

EUROPE CONGRESS
www.europecongress.org

TURKISH AIRLINES

CNR GROUP